Synthesis, Structure, Spectroscopy, and Reactivity of a Metallathiabenzene[1]

John R. Bleeke* and Paul V. Hinkle

Department of Chemistry, Washington University, One Brookings Drive, St. Louis, Missouri 63130

Nigam P. Rath

Department of Chemistry, University of Missouri−St. Louis, 8001 Natural Bridge Road, St. Louis, Missouri 63121

Received January 22, 2001

Treatment of $(Cl)Ir(PEt_3)_3$ with lithium 2,3-dimethyl-5-thiapentadienide leads to the production of *mer*-$\overline{CH{=}C(Me)C(Me){=}CHS}Ir(PEt_3)_3(H)$ (**4**) via C−H bond activation. Oxidation of **4** with silver tetrafluoroborate in tetrahydrofuran generates "iridathiabenzene", $[\overline{CH{=}C(Me)C(Me){=}CHS{=}}Ir(PEt_3)_3]^+BF_4^-$ (**3**). The structural and spectroscopic features of **3** are consistent with the presence of an aromatic ring in which the iridium center participates in ring π-bonding. Treatment of **3** with excess PMe_3 or with PPN^+Cl^- leads to the production of $\overline{CH{=}C(Me)C(Me){=}CHS}Ir(PMe_3)_4^+BF_4^-$ (**5**) or *mer*-$\overline{CH{=}C(Me)C(Me){=}CHS}Ir(PEt_3)_3(Cl)$ (**6**), respectively. Each of these products features an iridathiacyclohexa-1,3-diene ring system. The reaction of **6** with $^1/_2$ equiv of silver trifluoromethanesulfonate leads to the production of a novel iridium dimer, $[(\overline{CH{=}C(Me)C(Me){=}CHS}Ir(PEt_3)_2)_2(\mu\text{-}Cl)]^+O_3SCF_3^-$ (**7**), in which the two iridium centers are bridged by the two sulfur atoms of the iridathiacyclohexa-1,3-diene rings, as well as a chloride ligand. Treatment of **3** with nitrosobenzene generates a [4 + 2] cycloadduct, $[\overline{CH{=}C(Me)\underline{C(Me)CH{=}S}}IrON(Ph)](PEt_3)_3^+BF_4^-$ (**8**), containing an iridathiacyclohexa-1,4-diene ring. Compound **3** cleanly displaces *p*-xylene from (η^6-*p*-xylene)-$Mo(CO)_3$ in tetrahydrofuran, generating $[\eta^6\text{-}\overline{CH{=}C(Me)C(Me){=}CHS{=}}Ir(PEt_3)_3]Mo(CO)_3^+BF_4^-$ (**9**). When **9** is reacted with excess trimethylphosphine, PMe_3 adds to the molybdenum center, causing the iridathiabenzene ring to slip from η^6 to η^4 coordination and forming $[\eta^4\text{-}\overline{CH{=}C(Me)C(Me){=}CHS{=}}Ir(PEt_3)_2(CO)]Mo(PMe_3)_2(CO)_2^+BF_4^-$ (**10**). Finally, treatment of $(\eta^5\text{-}C_5Me_5)Ru(NCMe)_3^+O_3SCF_3^-$ with **3** leads to clean displacement of the acetonitrile ligands by the iridathiabenzene ring and generation of the Ru sandwich compound $[\eta^6\text{-}\overline{CH{=}C(Me)C(Me){=}CHS{=}}Ir(PEt_3)_3]Ru(\eta^5\text{-}C_5Me_5)^{2+}BF_4^-O_3SCF_3^-$ (**11**). Compounds **3**, **4**, **6a**, **7**, **9**, and **10** have been structurally characterized by X-ray diffraction.

Introduction

During the past decade, we have been studying the chemistry of the "iridabenzene" **1**,[2] a rare[3,4] metal-containing analogue of benzene. Our synthetic approach

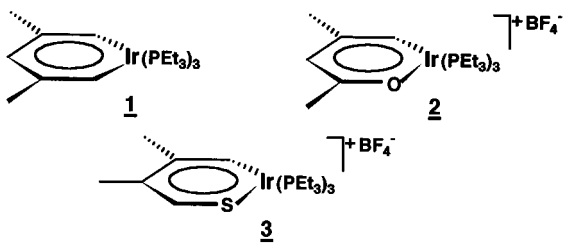

to this novel aromatic molecule involves use of a pentadienide reagent to supply the ring carbon atoms.

(1) Metallacyclohexadiene and Metallabenzene Chemistry. 17. Part 16: Bleeke, J. R.; Blanchard, J. M. B.; Donnay, E. *Organometallics* **2001**, *20*, 324.

(2) (a) Bleeke, J. R.; Xie, Y.-F.; Peng, W.-J.; Chiang, M. *J. Am. Chem. Soc.* **1989**, *111*, 4118. (b) Bleeke, J. R. *Acc. Chem. Res.* **1991**, *24*, 271. (c) Bleeke, J. R.; Behm, R.; Xie, Y.-F.; Chiang, M. Y.; Robinson, K. D.; Beatty, A. M. *Organometallics* **1997**, *16*, 606. (d) Bleeke, J. R.; Behm, R. *J. Am. Chem. Soc.* **1997**, *119*, 8503.

(3) For examples of other stable metallabenzenes, see: (a) Elliott, G. P.; Roper, W. R.; Waters, J. M. *J. Chem. Soc., Chem. Commun.* **1982**, 811. (b) Rickard, C. E. F.; Roper, W. R.; Woodgate, S. D.; Wright, L. J. *Angew. Chem., Int. Ed.* **2000**, *39*, 750. (c) Gilbertson, R. D.; Weakley, T. J. R.; Haley, M. M. *J. Am. Chem. Soc.* **1999**, *121*, 2597. (d) Gilbertson, R. D.; Weakley, T. J. R.; Haley, M. M. *Chem. Eur. J.* **2000**, *6*, 437.

(4) Detection of a thermally unstable metallabenzene at low temperature has also been reported: Yang, J.; Jones, W. M.; Dixon, J. K.; Allison, N. *J. Am. Chem. Soc.* **1995**, *117*, 9976.

10.1021/om010050s CCC: $20.00
Publication on Web 04/07/2001

Scheme 1

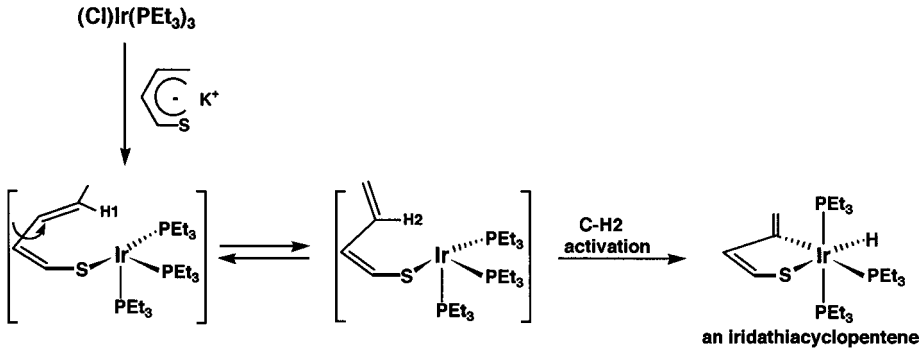

Scheme 2

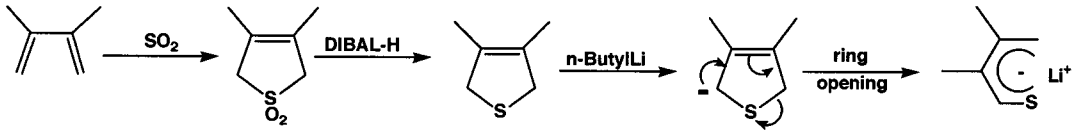

Scheme 3

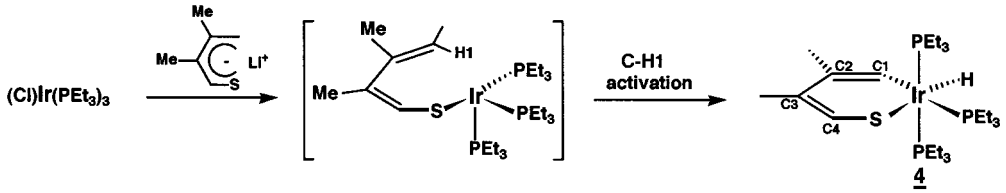

The key ring-forming step is metal-mediated activation of a pentadienyl C−H bond. Using a similar synthetic strategy, we have recently succeeded in producing an oxygen-containing relative of **1**, iridapyrylium **2**.[5] We now report that this same approach can be adapted to generate a sulfur-containing member of this unique aromatic family, iridathiabenzene **3**. In this paper, we describe the synthesis, structure, spectroscopy, and reaction chemistry of compound **3** and comment on the extent to which it exhibits aromatic character.[6]

It should be noted that several related examples of metallathiabenzenes have previously been reported. For example, Angelici[7] has synthesized iridathiabenzene **A**, while Jones[8] has reported the low-temperature detection of rhodium analogue **B**. Bianchini,[9] in turn, has gener-

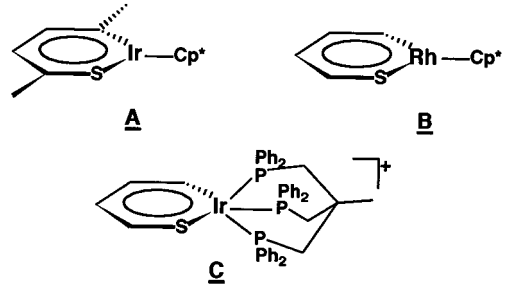

ated iridathiabenzene **C**, together with a close analogue containing a fused benzene ring. These previous syntheses differ from our approach in that they involve thiophene C−S bond activation as the key ring-forming step.[10]

Results and Discussion

A. Synthesis, Spectroscopy, and Structure of Iridathiabenzene 3. As shown in Scheme 1, we previously demonstrated that treatment of $(Cl)Ir(PEt_3)_3$ with unmethylated thiapentadienide leads to C−H2 bond activation and production of a five-membered metallacycle.[11]

To prevent this reaction pathway and promote six-membered-ring formation, we synthesized a new thiapentadienide reagent with methyl groups at the C2 and C3 positions. This synthesis, which culminates in base-initiated ring opening of the dimethyldihydrothiophene reagent, is summarized in Scheme 2.[12] As expected, treatment of $(Cl)Ir(PEt_3)_3$ with this new dimethylated

(5) (a) Bleeke, J. R.; Blanchard, J. M. B. *J. Am. Chem. Soc.* **1997**, *119*, 5443. (b) Bleeke, J. R.; Blanchard, J. M. B.; Donnay, E. *Organometallics* **2001**, *20*, 324.

(6) A portion of this work has been communicated: Bleeke, J. R.; Hinkle, P. V.; Rath, N. P. *J. Am. Chem. Soc.* **1999**, *121*, 595.

(7) (a) Chen, J.; Daniels, L. M.; Angelici, R. J. *J. Am. Chem. Soc.* **1990**, *112*, 199. (b) Chen, J.; Daniels, L. M.; Angelici, R. J. *Polyhedron* **1990**, *9*, 1883.

(8) Chin, R. M.; Jones, W. D. *Angew. Chem., Int. Ed. Engl.* **1992**, *31*, 357.

(9) (a) Bianchini, C.; Meli, A.; Peruzzini, M.; Vizza, F.; Frediani, P.; Herrera, V.; Sanchez-Delgado, R. A. *J. Am. Chem. Soc.* **1993**, *115*, 2731. (b) Bianchini, C.; Meli, A.; Peruzzini, M.; Vizza, F.; Moneti, S.; Herrera, V.; Sanchez-Delgado, R. A. *J. Am. Chem. Soc.* **1994**, *116*, 4370.

(10) Several other metal-mediated thiophene bond activations have led to metallathiacyclohexa-1,3-diene products. These molecules are related to metallathiabenzenes but do not exhibit the bond delocalization characteristic of aromatic species. See, for example: (a) Jones, W. D.; Dong, L. *J. Am. Chem. Soc.* **1991**, *113*, 559. (b) Selnau, H. E.; Merola, J. S. *Organometallics* **1993**, *12*, 1583. (c) Jones, W. D.; Chin, R. M.; Crane, T. W.; Baruch, D. M. *Organometallics* **1994**, *13*, 4448. (d) Buys, I. E.; Field, L. D.; Hambly, T. W.; McQueen, A. E. D. *J. Chem. Soc., Chem. Commun.* **1994**, 557. (e) Garcia, J. J.; Mann, B. E.; Adams, H.; Bailey, N. A.; Maitlis, P. M. *J. Am. Chem. Soc.* **1995**, *117*, 2179. (f) Arevalo, A.; Bernes, S.; Garcia, J. J.; Maitlis, P. M. *Organometallics* **1999**, *18*, 1680.

(11) (a) Bleeke, J. R.; Ortwerth, M. F.; Chiang, M. Y. *Organometallics* **1992**, *11*, 2740. (b) Bleeke, J. R.; Ortwerth, M. F.; Rohde, A. M. *Organometallics* **1995**, *14*, 2813.

(12) Kloosterziel first demonstrated the feasibility of this "cycloreversion" reaction: Kloosterziel, H.; Van Drunen, J. A. A.; Galama, P. *J. Chem. Soc. D* **1969**, 885.

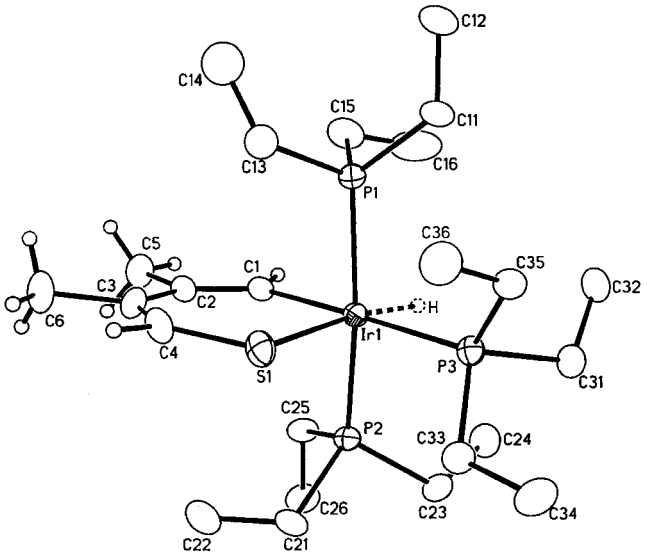

Figure 1. ORTEP drawing of *mer*-CH=C(Me)C(Me)=CHSIr(PEt_3)$_3$(H) (**4**), using thermal ellipsoids at the 20% probability level. The metal-bound hydrogen atom was placed at an idealized position but not refined. Selected bond distances (Å): Ir1−P1, 2.341(3); Ir1−P2, 2.341(3); Ir1−P3, 2.363(3); Ir1−S1, 2.433(3); Ir1−C1, 2.093(10); S1−C4, 1.731(12); C1−C2, 1.340(14); C2−C3, 1.456(18); C3−C4, 1.380(19). Selected bond angles (deg): P1−Ir1−P2, 159.9(1); P1−Ir1−P3, 101.5(1); P1−Ir1−S1, 97.0(1); P1−Ir1−C1, 79.8(3); P2−Ir1−P3, 94.6(1); P2−Ir1−S1, 95.4(1); P2−Ir1−C1, 84.4(3); P3−Ir1−S1, 88.3(1); P3−Ir1−C1, 178.5(3); S1−Ir1−C1, 90.8(3); Ir1−C1−C2, 133.7(8); C1−C2−C3, 127.4(10); C2−C3−C4, 126.7(10); C3−C4−S1, 130.8(10); C4−S1−Ir1, 110.1(4).

thiapentadienide reagent leads to the production of the desired six-membered metallacycle, iridathiacyclohexa-1,3-diene **4**, via C−H1 bond activation (Scheme 3).

The ^{1}H NMR spectrum of **4** exhibits downfield signals for ring protons H1 and H4 at δ 7.05 and 5.78, respectively, while the metal−hydride signal appears far upfield at δ −16.10. In the ^{13}C{^{1}H} NMR spectrum, the ring carbons resonate at δ 118.8 (C1), 127.3 (C2), 127.3 (C3), and 120.9 (C4). The signal for C1 is a characteristic doublet (J_{C-P} = 72.0 Hz) of triplets (J_{C-P} = 15.0 Hz) due to coupling to the ^{31}P nuclei of the *trans* equatorial and axial phosphines, respectively. The ^{31}P{^{1}H} NMR spectrum consists of a doublet of intensity 2 (axial phosphines) and a triplet of intensity 1 (equatorial phosphine).

The solid-state structure of **4**, determined by single-crystal X-ray diffraction, is shown in Figure 1; selected bond distances and angles are given in the figure caption. The structure confirms the octahedral coordination geometry and *mer* arrangement of the phosphine ligands. The metallacyclic ring is essentially planar and exhibits localized single and double bonds within the carbon/sulfur portion of the metallacycle. The Ir1−C1 and Ir1−S1 distances (2.093(10) and 2.433(3) Å, respectively) are typical single-bond lengths.[13]

Treatment of the yellow-orange iridathiacyclohexa-1,3-diene **4** with silver tetrafluoroborate in tetrahydrofuran leads to the immediate production of deep red iridathiabenzene **3**, presumably through the intermediacy of the 17e$^-$ oxidation product (see Scheme 4).[14] The ^{1}H NMR spectrum of **3** shows downfield shifting for ring protons H1 and H4, consistent with its formulation as an aromatic species. Proton H1 resonates at δ 10.36 and is a quartet (J_{H-P} = 8.4 Hz) due to coupling to three equivalent ^{31}P nuclei (vide infra), while H4 resonates at δ 8.61. The ring carbons resonate at δ 165.1 (C1), 143.6 (C2), 134.9 (C3), and 130.0 (C4), and C1 (like H1) appears as a phosphorus-coupled quartet (J_{C-P} = 21.6 Hz). The ^{31}P{^{1}H} NMR signal for **3**, like those for analogues **1**[2] and **2**,[5] is a singlet at room temperature, indicating that the three phosphine ligands are exchanging rapidly in solution. However, when the temperature is lowered to −90 °C, the ^{31}P{^{1}H} NMR signal broadens and ultimately resolves into two sharp resonances with an intensity ratio of 2:1. Simulation of the variable-temperature ^{31}P{^{1}H} NMR spectra yields a $\Delta G^{\ddagger}$ value of 9.5(0.2) kcal/mol for this intramolecular phosphine exchange process.[15]

The molecular structure of **3** has been determined by X-ray diffraction and is presented in Figure 2. Consistent with the low-temperature ^{31}P NMR spectrum described above, the molecule displays approximate (although not crystallographically imposed) mirror plane symmetry. The symmetry plane includes the metallacyclic ring and phosphorus atom P3, while bisecting the P1−Ir−P2 angle. The coordination geometry of the molecule is probably best described as a distorted trigonal bipyramid with C1 and P3 occupying the axial sites and S1, P1, and P2 occupying the equatorial sites. However, the equatorial ligands are significantly displaced from idealized positions. Hence, the three equatorial L−Ir−L angles, which ideally should each be 120°, are actually 136.8(1), 127.2(1), and 95.9(1)°. Surprisingly, the smallest of these angles involves the two bulky PEt_3 ligands![16]

Bonding within the metallacycle in **3** is delocalized, consistent with an aromatic system. The carbon−carbon bond distances C1−C2, C2−C3, and C3−C4 have moved toward equalization, while bonds Ir1−C1 and Ir1−S1 have both shortened substantially (vs their lengths in **4**), indicating significant metal participation in the ring π-bonding.[17] The nonmetal portion of the ring (C1/C2/C3/C4/S1) is very nearly planar (mean deviation 0.015 Å), while the iridium center lies 0.185 Å out of this plane. The dihedral angle between planes C1/C2/C3/C4/S1 and C1/Ir1/S1 is 7.0°.

B. Reactivity of Iridathiabenzene 3: Addition to the Iridium Center. One can write three reasonable

(13) Orpen, A. G.; Brammer, L.; Allen, F. H.; Kennard, O.; Watson, D. G.; Taylor, R. *J. Chem. Soc., Dalton Trans* **1989**, S1.

(14) The fate of the metal-bound hydrogen is not known.

(15) The exchange probably proceeds via a Berry pseudorotation or a turnstile mechanism: Cotton, F. A.; Wilkinson, G. *Advanced Inorganic Chemistry*, 4th ed.; Wiley: New York, 1980; pp 1218−1220.

(16) Iridabenzene **1** adopts a coordination geometry in the solid state that is best described as square pyramidal. It also exhibits approximate mirror plane symmetry, but in this case the symmetry plane bisects the metallacyclic ring.[2]

(17) According to recent Fenske−Hall MO calculations by Harris, the key orbital interaction involves the filled 3π orbital on the thiapentadienyl moiety, which is centered largely on sulfur, and on an empty metal d orbital of appropriate symmetry. Overlap between these orbitals produces a filled bonding MO with significant Ir−S π character, as well as the molecule's LUMO, which is primarily metal in character. See: (a) Harris, S. *Organometallics* **1994**, *13*, 2628. (b) Palmer, M.; Carter, K.; Harris, S. *Organometallics* **1997**, *16*, 2448. (c) Blonski, C.; Myers, A. W.; Palmer, M.; Harris, S.; Jones, W. D. *Organometallics* **1997**, *16*, 3819.

Scheme 4

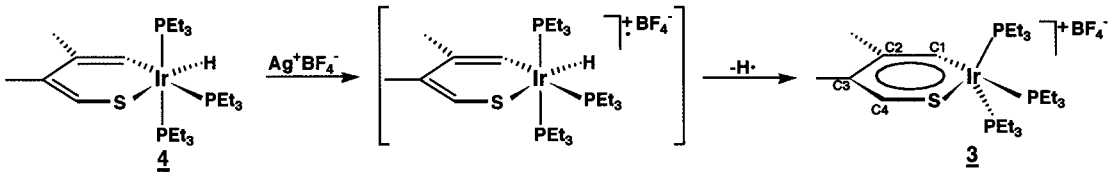

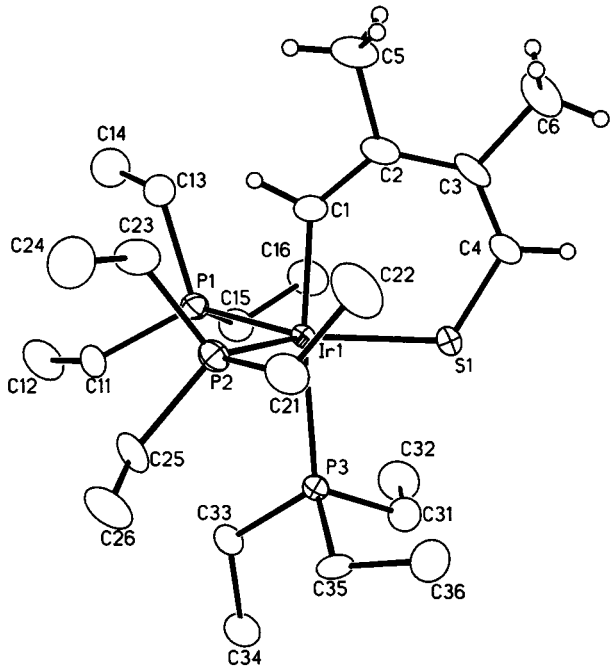

Figure 2. ORTEP drawing of CH=C(Me)C(Me)=CHS=Ir-$(PEt_3)_3{}^+BF_4{}^-$ (**3**), using thermal ellipsoids at the 20% probability level. Selected bond distances (Å): Ir1−P1, 2.305(3); Ir1−P2, 2.275(3); Ir1−P3, 2.450(3); Ir1−S1, 2.249(3); Ir1−C1, 2.019(10); S1−C4, 1.713(12); C1−C2, 1.396(16); C2−C3, 1.415(15); C3−C4, 1.361(16). Selected bond angles (deg): P1−Ir1−P2, 95.9(1); P1−Ir1−P3, 97.5(1); P1−Ir1−S1, 136.8(1); P1−Ir1−C1, 88.8(3); P2−Ir1−P3, 95.5(1); P2−Ir1−S1, 127.2(1); P2−Ir1−C1, 88.3(3); P3−Ir1−S1, 83.0(1); P3−Ir1−C1, 172.3(3); S1−Ir1−C1, 89.3(3); Ir1−C1−C2, 134.1(8); C1−C2−C3, 126.7(10); C2−C3−C4, 125.0(11); C3−C4−S1, 127.7(9); C4−S1−Ir1, 116.4(4).

resonance structures for iridathiabenzene **3** (**D**−**F**). In

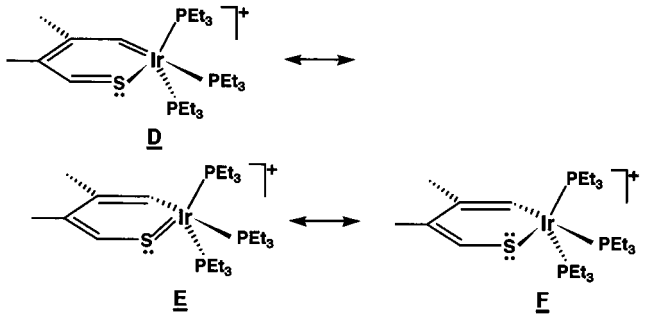

structures **D** and **E**, the iridium center possesses 18 valence electrons, while in **F** it possesses 16 electrons. Structures **E** and **F** differ only in the position of one electron pair. In **E**, it resides between sulfur and iridium, forming the π bond, while in **F** it resides on the sulfur atom.[18] Because of the contribution from resonance structure **F**, the iridium atom in **3** is reactive toward 2e$^-$ donor ligands, leading to the formation of six-coordinate iridathiacyclohexa-1,3-diene compounds.[19]

For example, treatment of **3** with excess trimethylphosphine at 22 °C leads to PMe_3 addition at the iridium center *and* complete replacement of the three bulky PEt_3 ligands with PMe_3's, generating the tetrakis(trimethylphosphine) product **5** (Scheme 5). This reaction contrasts sharply with the room-temperature reaction of iridabenzene **1** with excess PMe_3, which results in replacement of just one PEt_3 ligand with PMe_3 and retention of the aromatic ring system.[2] The reason for this difference in behavior is that **1** reacts with PMe_3 by a *dissociative* mechanism (i.e., PEt_3 must dissociate before PMe_3 can add), while **3** reacts with PMe_3 in an *associative* fashion (see Scheme 6). This associative mechanism is made possible by the fact that the Ir−S π electrons can be localized on the sulfur atom (cf., resonance structure **F**), rendering the iridium atom a reactive 16e$^-$ center.

The $^{31}P\{^1H\}$ NMR spectrum of **5** consists of three signals—a doublet of doublets due to the two equivalent axial phosphines and two triplets of doublets due to the inequivalent equatorial phosphines. In the $^{13}C\{^1H\}$ NMR spectrum, ring carbons C1−C4 resonate in a rather narrow chemical shift range, δ 115.8−132.0, and the signal for C1 is a doublet-of-triplets-of-doublets pattern. The large doublet coupling (J_{C-P} = 70.5 Hz) is due to the *trans*-equatorial phosphine, while the smaller triplet (J_{C-P} = 12.0 Hz) and doublet (J_{C-P} = 6.0 Hz) couplings result from the axial and *cis*-equatorial phosphines, respectively. In the ^1H NMR spectrum, ring protons H1 and H4 resonate at δ 6.85 and 5.54, respectively, and both exhibit strong coupling to the *cis*-equatorial PMe_3 ligand (J_{H1-P} = 14.7 Hz; J_{H4-P} = 14.1 Hz).

When iridathiabenzene **3** is treated with bis(triphenylphosphoranylidene)ammonium chloride (PPN^+Cl^-), the chloride addition product, *mer*-CH=C(Me)C(Me)=CHSIr$(PEt_3)_3$(Cl), is generated as a mixture of isomers, **6a** and **6b** (see Scheme 5). Isomer **6a** can be crystallized cleanly from this mixture and exhibits NMR spectra that are very similar to those of hydride **4**. In particular, the $^{31}P\{^1H\}$ NMR spectrum of **6a** consists of a doublet and a triplet characteristic of an octahedral coordination geometry and a *mer* phosphine arrangement. The *trans* relationship of ring carbon C1 to a phosphine ligand is indicated by the large C−P coupling (J_{C-P} = 84.0 Hz).

The solid-state structure of **6a** has been confirmed by X-ray crystallography (see Figure 3). As expected, the metallacycle is virtually planar and exhibits localized

(18) Note that in structures **D** and **E**, the formal positive charge resides on sulfur, while in **F** it resides on the iridium center.

(19) Analogous iridathiabenzene reactivity toward 2e$^-$ donor ligands has been observed by Angelici[7b] and Bianchini.[9] Harris[16] has attributed this reactivity to a low-lying metal-based LUMO.

Scheme 5

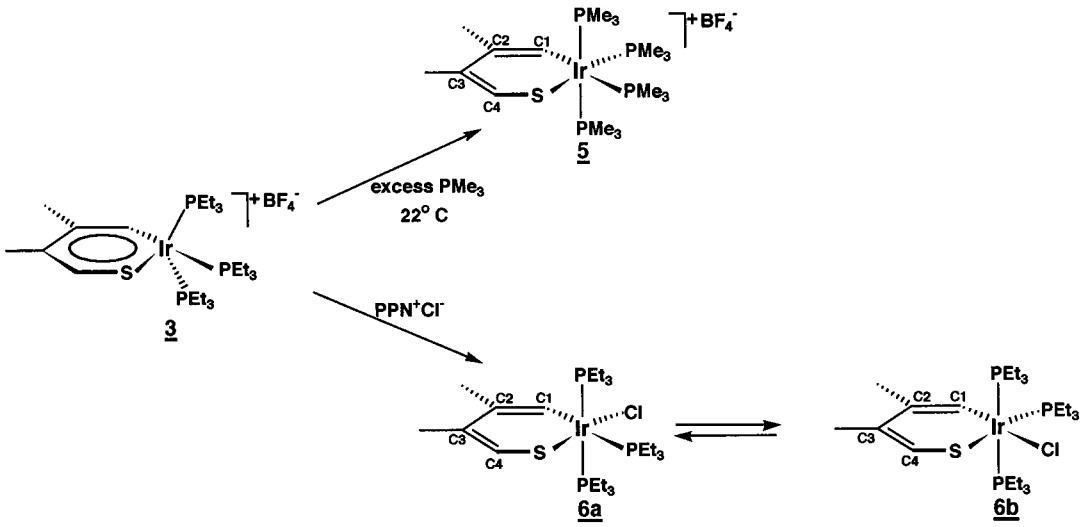

Scheme 6

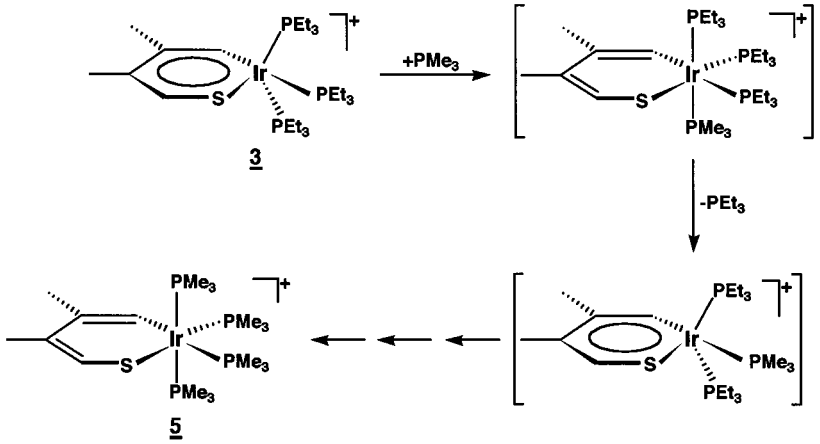

bonding around the carbon/sulfur portion of the ring. The Ir1−S1 bond in **6a** (2.321(3) Å) is somewhat shorter than the Ir1−S1 bond in **4** (2.433(3) Å), reflecting the weaker *trans* influence of chloride.[20]

When crystalline **6a** (light orange) is dissolved in polar solvents such as acetone, it gives a deep red solution, and it rapidly establishes an equilibrium with compound **6b**, the isomer in which PEt_3 and Cl^- have exchanged positions in the equatorial plane.[21] At room temperature in acetone, the equilibrium ratio **6a**:**6b** is approximately 60:40.

Once again, the arrangement of the ligands in **6b** can be readily established by NMR. The $^{31}P\{^1H\}$ NMR spectrum consists of a doublet and a triplet, diagnostic for *mer* phosphines. However, ring carbon C1 shows no strong phosphorus coupling in the $^{13}C\{^1H\}$ NMR, indicating that it resides *trans* to chloride, not to a PEt_3 ligand. Furthermore, ring protons H1 and H4 are both strongly phosphorus coupled ($J_{H1-P} = 14.7$ Hz; $J_{H4-P} = 13.2$ Hz), confirming the presence of a PEt_3 ligand *cis* to C1 in the equatorial plane.

As shown in Scheme 7, we suggest that the isomerization process proceeds through the intermediacy of iridathiabenzenes **G** and **H** and that these species are responsible for the intense red color of the solutions.[22] Interestingly, the NMR signals for **6b** are very broad at room temperature (22 °C) and do not fully sharpen until a temperature of −20 °C is reached. This behavior suggests a rapid equilibrium with intermediate **H** (Scheme 7) at 22 °C. The NMR signals for **6a**, on the other hand, are sharp at 22 °C but begin to broaden as the temperature is raised. At 40 °C, P−P coupling is lost in the $^{31}P\{^1H\}$ NMR spectrum of **6a**.

We expected that treatment of **6a**/**6b** in acetone with silver trifluoromethanesulfonate might lead to chloride abstraction and regeneration of iridathiabenzene **3**. In fact, $^1/_2$ equiv of silver chloride is produced in this reaction, but the organometallic product is a novel chloride-bridged dimer, **7** (see Scheme 8), not the expected **3**.

Although the detailed mechanism of this reaction is not known, it seems likely that the dimerization proceeds through the intermediacy of the five-coordinate iridathiabenzene species **H** implicated earlier in the isomerization of **6a** to **6b** (cf. Scheme 7). As shown in Scheme 8, dimerization of **H** through the ring sulfur

(20) Huheey, J. E.; Keiter, E. A.; Keiter, R. L. *Inorganic Chemistry: Principles of Structure and Reactivity*, 4th ed.; HarperCollins: New York, 1993; pp 543−547.

(21) A close analogue of this species with PMe_3 ligands has been reported by Merola.[10b]

(22) We can rule out the intermediacy of iridathiabenzene **3** in this reaction because addition of excess PMe_3 to the red solution does *not* yield the cationic tetrakis(trimethylphosphine) product **5**. Rather, neutral chloro-containing substitution products are obtained.

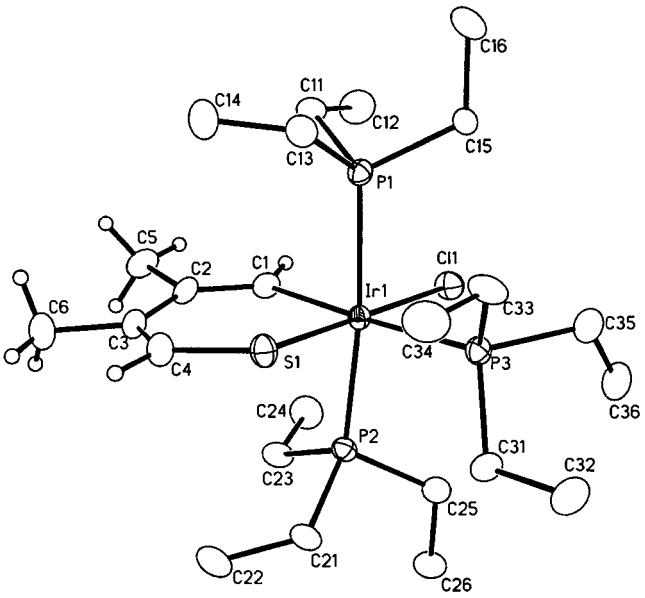

Figure 3. ORTEP drawing of *mer*-CH=C(Me)C(Me)=CHSIr(PEt_3)$_3$(Cl) (**6a**), using thermal ellipsoids at the 20% probability level. Selected bond distances (Å): Ir1−Cl1, 2.445(3); Ir1−P1, 2.375(3); Ir1−P2, 2.374(3); Ir1−P3, 2.430(3); Ir1−S1, 2.321(3); Ir1−C1, 2.055(10); S1−C4, 1.741(12); C1−C2, 1.352(16); C2−C3, 1.470(17); C3−C4, 1.334(17). Selected bond angles (deg): Cl1−Ir1−P1, 86.6(1); Cl1−Ir1−P2, 89.8(1); Cl1−Ir1−P3, 92.8(1); Cl1−Ir1−S1, 180.0(1); Cl1−Ir1−C1, 87.7(3); P1−Ir1−P2, 169.2(1); P1−Ir1−P3, 94.0(1); P1−Ir1−S1, 93.4(1); P1−Ir1−C1, 82.9(3); P2−Ir1−P3, 96.4(1); P2−Ir1−S1, 90.3(1); P2−Ir1−C1, 86.8(3); P3−Ir1−S1, 87.2(1); P3−Ir1−C1, 176.8(3); S1−Ir1−C1, 92.3(3); Ir1−C1−C2, 133.3(9); C1−C2−C3, 125.6(11); C2−C3−C4, 125.9(11); C3−C4−S1, 131.9(10); C4−S1−Ir1, 109.9(4).

Scheme 7

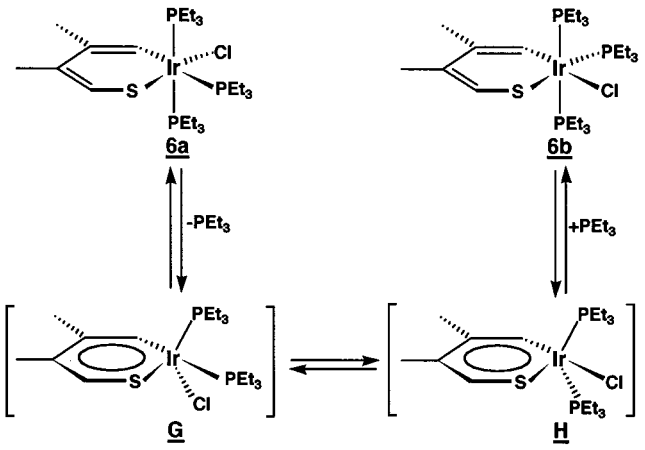

centers would lead to dimer **I**, which could then react with AgO_3SCF_3 to generate **7** and AgCl.

The structure of **7** has been confirmed by X-ray diffraction. An ORTEP drawing is presented in Figure 4. Each of the iridium centers in **7** is approximately octahedral, and in each case, the four equatorial sites are occupied by the metallacycle, a PEt_3 ligand, and the bridging chloride. The sulfur atom from the neighboring ring and a second PEt_3 ligand occupy the axial sites. The bridging chloride ligand resides *cis* to the ring sulfur and *trans* to the ring carbon in both equatorial planes.

The chloride bridge is symmetrical with respect to the two iridium centers, while the sulfur bridges are unsymmetrical. The iridium−sulfur distances within the metallacycles (average 2.37 Å) are shorter than those to sulfur atoms on neighboring rings (average 2.43 Å). The bond distances and angles within the iridathiacyclohexa-1,3-diene rings in **7** are similar to those observed in **6a**. However, a close comparison reveals that the Ir−C bonds in **7** (2.014(12) and 2.039(15) Å) are slightly shorter than the Ir−C bond in **6a** (2.055(10) Å), probably reflecting the weaker *trans* influence of chloride vs PEt_3.[20] Consistent with this interpretation is the observation that the Ir−S bonds within the metallacycles of **7** are slightly longer than the Ir−S bond in **6a** (2.376(3) and 2.364(3) Å in **7** vs 2.321(3) Å in **6a**). The presence of the bridging chloride ligand causes the rings to twist out of register, so that they do not exactly eclipse one another. In addition, the rings are slightly canted, instead of being parallel. The dihedral angle between the two metallacycle mean planes is 25.9°.

Compound **7** possesses 2-fold rotation symmetry in solution; therefore, the two metallacyclic rings appear equivalent by ^{1}H and ^{13}C{^{1}H} NMR. The H1 and H4 protons resonate at δ 8.07 and 5.51, respectively, and both are strongly coupled doublets due to the presence of a phosphine ligand *cis* to C1 in the equatorial plane (J_{H1-P} = 9.9 Hz; J_{H4-P} = 11.7 Hz). The ring carbons resonate in the expected region of the ^{13}C NMR spectrum (δ 107.1−141.7), and C1 is not strongly coupled to phosphorus, because it lies *trans* to chloride rather than PEt_3.

The ^{31}P{^{1}H} spectrum of **7** is a classic AA′XX′ second-order pattern. This results from the fact that each iridium center has two kinds of phosphine ligands, an A type and an X type, and although the two A-type ligands are chemically equivalent (as are the two X-type ligands), they are not magnetically equivalent due to long-range coupling. The A-type phosphines and the X-type phosphines each give rise to identical 10-line patterns at δ −12.9 and −17.6, respectively. Each pattern consists of a strong doublet, which is centered on the frequency of δ_A (or δ_X), and two symmetrical quartets, which are likewise centered on δ_A (or δ_X) (see Figure 5). From the separation between the various lines, one can calculate all of the coupling constants.[23] In this case, $J_{AA'}$ and $J_{XX'}$ are calculated to be 27.5 and 14.3 Hz, while J_{AX} and $J_{AX'}$ are 17.9 and 3.3 Hz.[24]

C. Reactivity of Iridathiabenzene 3: Cycloaddition.[25] Both iridabenzene **1**[2] and iridapyrylium **2**[5] react with a wide variety of unsaturated substrates to produce [4 + 2] cycloadducts. Although iridathiabenzene **3** seems to be less prone to exhibit this type of reactivity, we have discovered one such cycloaddition reaction, namely the reaction of **3** with nitrosobenzene to produce **8** (Scheme 9). The iridathiacyclohexa-1,4-diene ring in **8** is char-

(23) (a) Pople, J. A.; Schneider, W. G.; Bernstein, H. J. *High-Resolution Nuclear Magnetic Resonance*; McGraw-Hill: New York, 1959, pp 140−151. (b) Wiberg, K. B.; Nist, B. J. *The Interpretation of NMR Spectra*; W. A. Benjamin: New York, 1962; pp 309−317.

(24) From the data analysis, one cannot distinguish between $J_{AA'}$ and $J_{XX'}$ nor between J_{AX} and $J_{AX'}$.

(25) For a good summary of cycloaddition reactions involving organic components, see: Lowry, T. H.; Richardson, K. S. *Mechanism and Theory in Organic Chemistry*, 3rd ed.; Harper and Row: New York, 1987; pp 903−931.

Scheme 8

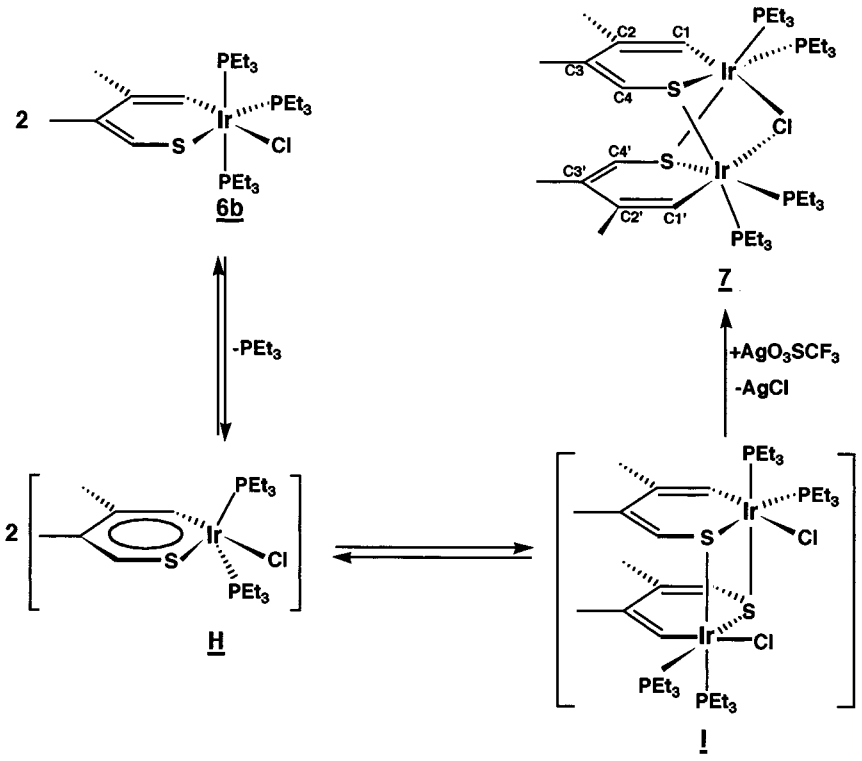

acterized by a relatively upfield ^{13}C NMR chemical shift for sp^3 carbon C3 (δ50.8) and a corresponding downfield shift for thioaldehyde carbon C4 (δ154.2). Olefinic carbons C1 and C2 resonate at δ 136.4 and 149.6, respectively, and C1 exhibits strong phosphorus coupling due to the *trans* PEt_3 ligand (J_{C-P} = 93.0 Hz). In the ^1H NMR spectrum, the signal for thioaldehyde proton H4 appears downfield at δ 8.31, while the ring proton H1 resonates at δ 6.79 and appears as a phosphorus-coupled triplet (J_{H-P} = 10.0 Hz). The $^{31}P\{^1H\}$ spectrum consists of three separate doublet-of-doublet patterns, consistent with a *fac* geometry for the three PEt_3 ligands.

D. Reactivity of Iridathiabenzene 3: Coordination to Other Metal−Ligand Fragments. Earlier, we showed that iridabenzene **1** could be coordinated to a $Mo(CO)_3$ fragment to produce (η^6-iridabenzene)$Mo(CO)_3$.[26] Similarly, treatment of **3** with (η^6-*p*-xylene)$Mo(CO)_3$ in tetrahydrofuran leads to arene exchange and clean production of the deep violet (η^6-iridathiabenzene)-$Mo(CO)_3$ species **9** (Scheme 10).[27]

The NMR signals for the ring protons and carbons in **9** shift upfield from their positions in **3**, as is normally observed when arenes π-coordinate to transition metals.[28] Protons H1 and H4 in **9** resonate at δ 8.27 and 6.59, respectively, and are strongly coupled to the basal phosphine that resides *cis* to C1. Carbons C1, C2, C3, and C4 resonate at δ 129.0, 117.6, 109.5, and 89.0, respectively, and C1 exhibits strong coupling to the ^{31}P nucleus that lies *trans* to it (J_{C-P} = 61.8 Hz). Unlike **3**, which undergoes intramolecular phosphine exchange in solution at room temperature (vide supra), **9** is stereochemically rigid. Hence, the $^{31}P\{^1H\}$ NMR spectrum at 22 °C consists of three discrete signals for the three inequivalent phosphine ligands. However, the $^{13}C\{^1H\}$ NMR spectrum of **9** exhibits a single peak for the three carbonyl ligands (at δ 220.9), indicating that the iridathiabenzene ring is rotating freely with respect to the $Mo(CO)_3$ moiety.

The infrared spectrum of **9** shows the presence of two intense ν(CO) bands (A_1 and E) at 1962 and 1895 cm^{-1}. By comparison, the ν(CO) bands for (η^6-iridabenzene)-$Mo(CO)_3$ appear at 1918 and 1836 cm^{-1}. The higher energy of the bands in **9** reflects the positive charge on **9** and, consequently, the reduced π-back-bonding into CO π^* orbitals.

The X-ray crystal structure of **9** (see Figure 6) shows that the molybdenum atom is strongly π-complexed to all six atoms of the iridathiabenzene ring and that the bonding within this ring is still delocalized. However, the bond lengths in the complexed ring are slightly longer than those in the free iridathiabenzene, because π-electron density is being removed from the ring by the $Mo(CO)_3$ moiety. The circumference of the ring in **3** is 10.15 Å, while that in **9** is 10.37 Å. The metallacyclic ring in **9** is close to planar. The iridium atom is displaced 0.21 Å out of the carbon/sulfur ring plane (and away from Mo). The dihedral angle between the planes C1/C2/C3/C4/S and C1/Ir/S is 7.7°.

The coordination geometry at the iridium center in **9** is best described as a square pyramid, where atoms C1, S, P2, and P3 define the basal ligand set while phosphorus atom P1 occupies the unique axial site. This shift in coordination geometry from a distorted trigonal

(26) Bleeke, J. R.; Bass, L. A.; Xie, Y.-F.; Chiang, M. Y. *J. Am. Chem. Soc.* **1992**, *114*, 4213.
(27) Angelici has also coordinated his iridathiabenzene to $M(CO)_3$ fragments, where M = Cr, Mo, W: Chen, J.; Young, V. G., Jr.; Angelici, R. J. *J. Am. Chem. Soc.* **1995**, *117*, 6362.
(28) Collman, J. P.; Hegedus, L. S.; Norton, J. R.; Finke, R. G. *Principles and Applications of Organotransition Metal Chemistry*; University Science Books: Mill Valley, CA, 1987; pp 158−164.

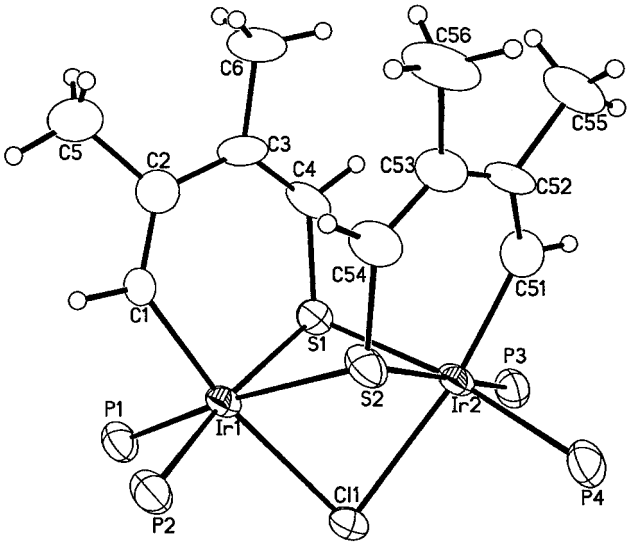

Figure 4. ORTEP drawing of $[(\overline{CH{=}C(Me)C(Me){=}CHS}Ir(PEt_3)_2)_2(\mu\text{-}Cl)]^+O_3SCF_3^-$ (**7**) with ethyl groups removed from PEt_3 ligands for clarity. Thermal ellipsoids are shown at the 50% probability level. Selected bond distances (Å): Ir1−Cl1, 2.559(3); Ir1−P1, 2.320(3); Ir1−P2, 2.329(3); Ir1−S2, 2.434(3); Ir1−S1, 2.376(3); Ir1−C1, 2.014(12); S1−C4, 1.753(14); C1−C2, 1.359(18); C2−C3, 1.445(19); C3−C4, 1.358(18); Ir2−Cl1, 2.542(3); Ir2−P3, 2.324(3); Ir2−P4, 2.320(4); Ir2−S1, 2.432(3); Ir2−S2, 2.364(3); Ir2−C51, 2.039(15); S2−C54, 1.732(14); C51−C52, 1.34(2); C52−C53, 1.46(2); C53−C54, 1.351(19). Selected bond angles (deg): P1−Ir1−S2, 169.98(12); P2−Ir1−S1, 167.79(12); Cl1−Ir1−C1, 170.1(3); S1−Ir1−C1, 92.7(4); Ir1−C1−C2, 129.9(9); C1−C2−C3, 128.0(12); C2−C3−C4, 125.7(12); C3−C4−S1, 129.4(10); C4−S1−Ir1, 106.5(4); Ir1−C11−Ir2, 82.24(8); Ir1−S1−Ir2, 88.51(11); Ir1−S2−Ir2, 88.74(11); P3−Ir2−S2, 171.15(12); P4−Ir2−S1, 170.84(12); Cl1−Ir2−C51, 167.6(4); S2−Ir2−C51, 92.5(4); Ir2−C51−C52, 131.6(12); C51−C52−C53, 127.6(13); C52−C53−C54, 128.0(13); C53−C54−S2, 128.3(12); C54−S2−Ir2, 110.6(5).

bipyramid in **3** to a square pyramid in **9** is undoubtedly a response to the steric demands of the $Mo(CO)_3$ moiety.

Treatment of **9** with PMe_3 leads to the production of a novel η^4-iridathiabenzene complex **10** (see Scheme 10). In this product, two PMe_3 ligands have been added to the molybdenum center and a CO ligand (formerly bonded to Mo) has replaced a PEt_3 ligand on iridium. To accommodate the two PMe_3 and two CO ligands while retaining an $18e^-$ count, the molybdenum center shifts to an η^4 interaction with the iridathiabenzene ring.

The ^1H NMR signals for ring protons H1 and H4 in **10** are shifted upfield from their position in **9**, reflecting the disruption of the aromatic ring system. They resonate at δ 7.60 and 5.92, respectively (vs δ 8.27 and 6.59 in **9**), and both are singlets due to the absence of a phosphine *cis* to C1 in the basal plane. In the $^{13}C\{^1H\}$ NMR spectrum of **10**, the two CO ligands on molybdenum resonate at δ 235.0 and 232.1, respectively, while the CO on iridium resonates farther upfield at δ 176.7. Interestingly, all of the ring carbon signals shift downfield with respect to their positions in **9**. As in **9**, C1 is strongly coupled to the *trans* PEt_3 ligand (J_{C-P} = 70.3 Hz). All four phosphine ligands give rise to discrete signals in the $^{31}P\{^1H\}$ NMR. The two PMe_3 ligands on

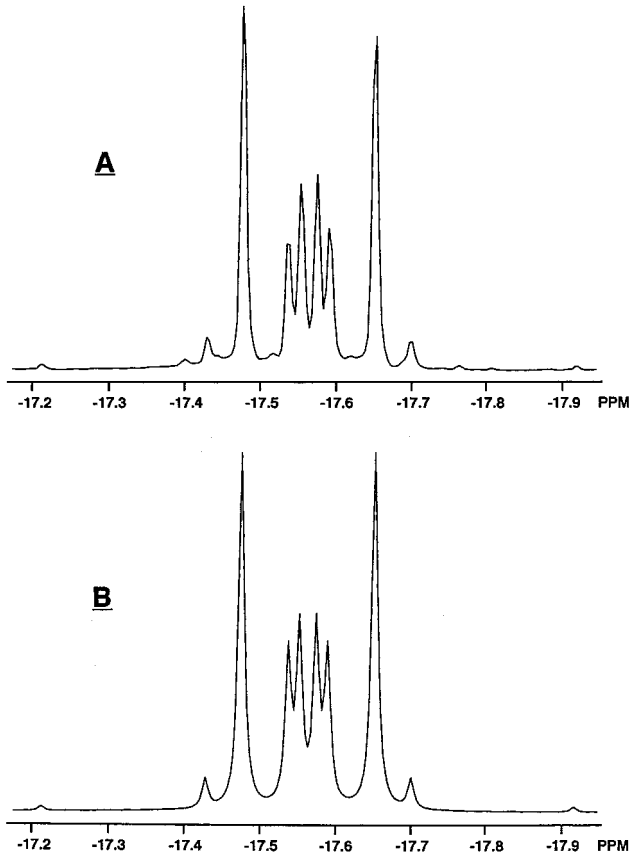

Figure 5. (A) Portion of the observed $^{31}P\{^1H\}$ NMR spectrum for $[(\overline{CH{=}C(Me)C(Me){=}CHS}Ir(PEt_3)_2)_2(\mu\text{-}Cl)]^+O_3SCF_3^-$ (**7**). Shown here is the 10-line signal due to the two X-type phosphines in this AA′XX′ spin system. The signal due to the two A-type phosphines (δ −12.9) is identical. (B) Simulated spectrum for the X-type phosphines in **7**, obtained using the following P−P coupling constants: $J_{AA'}$ = 27.5 Hz, $J_{XX'}$ = 14.3 Hz, J_{AX} = 17.9 Hz, $J_{AX'}$ = 3.3 Hz.

Scheme 9

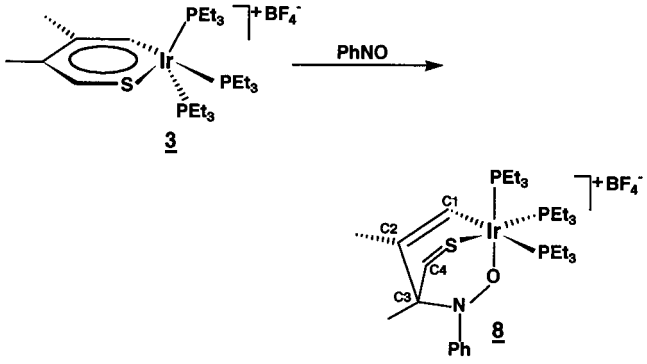

molybdenum couple strongly to each other (J_{P-P} = 43.2 Hz), and one of them shows a long-range coupling to the axial PEt_3 ligand on iridium (J_{P-P} = 14.5 Hz).

The X-ray crystal structure of **10** is shown in Figure 7. The molybdenum center is coordinated in an η^4 fashion to an iridathiadiene fragment consisting of S, Ir, C1, and C2. In response to this coordination mode, the ring adopts a bent conformation in which uncoordinated carbons C3 and C4 are displaced away from the molybdenum center. The dihedral angle between planes

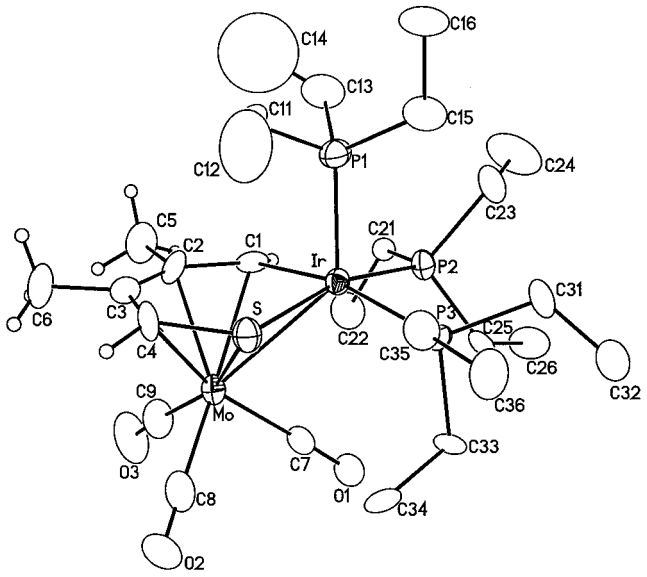

Figure 6. ORTEP drawing of [η^6-CH=C(Me)C(Me)=CHS=Ir(PEt_3)$_3$]Mo$(CO)_3^+BF_4^-$ (**9**), using thermal ellipsoids at the 40% probability level. Compound **9** crystallized with two independent molecules in the unit cell; molecule 1 is reported here. Selected bond distances (Å): Ir−P1, 2.274(5); Ir−P2, 2.371(5); Ir−P3, 2.424(4); Ir−S, 2.312(4); Ir−C1, 2.049(15); S−C4, 1.766(16); C1−C2, 1.42(2); C2−C3, 1.40(3); C3−C4, 1.42(2); Mo−Ir, 3.0180(16); Mo−S, 2.544(5); Mo−C1, 2.459(16); Mo−C2, 2.382(19); Mo−C3, 2.399(18); Mo−C4, 2.382(17); Mo−C7, 1.968(19); Mo−C8, 2.01(2); Mo−C9, 2.01(2). Selected bond angles (deg): P1−Ir−P2, 96.13(17); P1−Ir−P3, 101.54(16); P1−Ir−S, 99.49(19); P1−Ir−C1, 90.6(4); P2−Ir−P3, 92.42(15); P2−Ir−S, 164.37(18); P2−Ir−C1, 90.1(6); P3−Ir−S, 84.59(15); P3−Ir−C1, 167.2(4); S−Ir−C1, 89.6(6); Ir−C1−C2, 135.5(15); C1−C2−C3, 126.5(17); C2−C3−C4, 125.3(16); C3−C4−S, 128.1(13); C4−S−Ir, 114.0(7); C1−Mo−C8, 167.2(8); C3−Mo−C7, 160.6(7); S−Mo−C9, 161.7(5).

Scheme 10

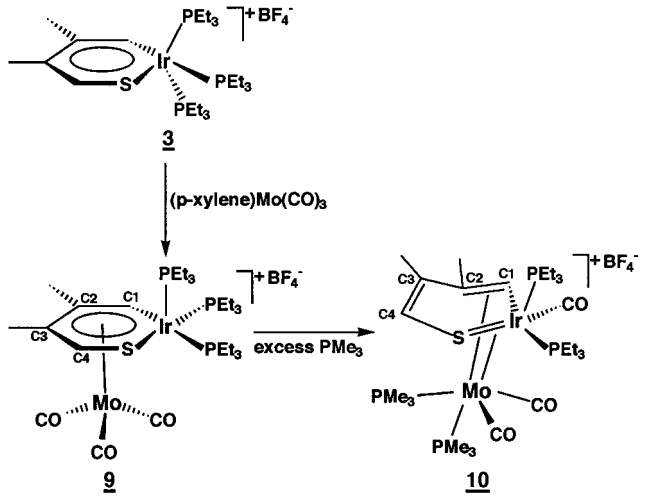

C2/C3/C4/S and S/Ir/C1/C2 is 46.7°. Disruption of the aromaticity in the iridathiabenzene ring also causes the ring bonding to become much more localized. This is particularly evident in the ring C−C bond distances, which are 1.35(3), 1.52(3), and 1.37(3) Å for C1−C2, C2−C3, and C3−C4, respectively. The Ir−S distance of 2.362(4) Å is a bit longer than might be expected from

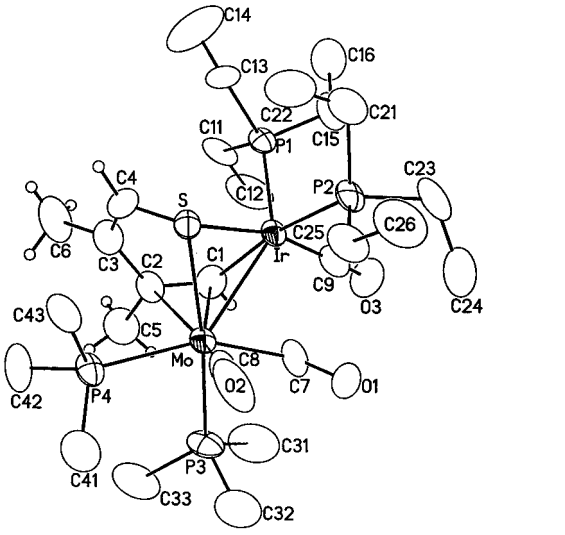

Figure 7. ORTEP drawing of [η^4-CH=C(Me)C(Me)=CHS=Ir(PEt_3)$_2$(CO)]Mo$(PMe_3)_2(CO)_2^+BF_4^-$ (**10**), using thermal ellipsoids at the 50% probability level. Selected bond distances (Å): Ir−P1, 2.330(5); Ir−P2, 2.402(4); Ir−C9, 1.88(2); Ir−S, 2.362(4); Ir−C1, 2.061(19); S−C4, 1.74(2); C1−C2, 1.35(3); C2−C3, 1.52(3); C3−C4, 1.37(3); Mo−Ir, 2.8586(16); Mo−S, 2.500(4); Mo−C1, 2.413(17); Mo−C2, 2.618(18); Mo−P3, 2.483(5); Mo−P4, 2.542(5); Mo−C7, 1.970(19); Mo−C8, 1.934(19). Selected bond angles (deg): P1−Ir−P2, 98.11(16); P1−Ir−C9, 93.3(6); P1−Ir−S, 100.06(16); P1−Ir−C1, 96.5(5); P2−Ir−C9, 94.4(5); P2−Ir−S, 90.06(16); P2−Ir−C1, 165.1(5); C9−Ir−S, 165.2(6); C9−Ir−C1, 88.1(7); S−Ir−C1, 84.2(5); Ir−C1−C2, 132.8(14); C1−C2−C3, 122.0(17); C2−C3−C4, 121.1(16); C3−C4−S, 122.1(15); C4−S−Ir, 105.8(6); S−Mo−P3, 168.22(18); C7−Mo−P4, 150.8(6); C1−Mo−C8, 158.0(7); C2−Mo−C8, 162.1(7).

resonance structure **J** (cf. the Ir−S distance of 2.312(4) Å in **9**). This suggests that a second resonance structure

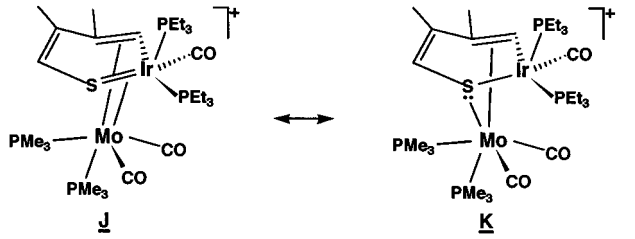

(**K**) involving coordination of a sulfur lone pair rather than the Ir−S double bond may also contribute to the overall bonding picture in **10**. This view is further supported by the observation that the angle at S (angle Ir−S−C4) in **10** is significantly smaller than the same angle in **9** (105.8(6) vs 116.4(4)°). As in **9**, the coordination geometry around iridium is best described as square pyramidal with ring atoms C1 and S, carbonyl carbon C9, and phosphorus P2 occupying the basal positions and phosphorus P1 occupying the unique axial site.

Finally, treatment of iridathiabenzene **3** with (η^5-pentamethylcyclopentadienyl)Ru$(NCMe)_3^+O_3SCF_3^-$ leads to clean acetonitrile displacement and production of "sandwich" complex **11** (Scheme 11). The ^{1}H NMR spectrum of **11** is strikingly similar to that of **9**.

Iridathiabenzene ring protons H1 and H4 resonate at δ 8.83 and 6.33, respectively, and each exhibits strong

Scheme 11

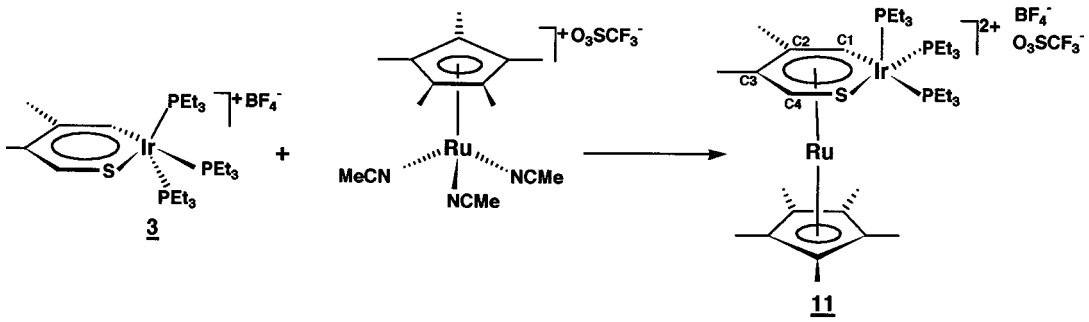

coupling to the PEt_3 ligand that resides *cis* to C1 in the basal plane of iridium (J_{H1-P} = 15.6 Hz; J_{H4-P} = 9.0 Hz). The chemical shifts of the iridathiabenzene ring carbons are also similar to those of **9**. C1, C2, C3, and C4 resonate at δ 116.8, 110.6, 100.5, and 77.9, respectively, and C1 shows strong coupling to the *trans*-basal PEt_3 ligand (J_{C-P} = 62.7 Hz). In the $^{31}P\{^1H\}$ NMR spectrum of **11**, three separate signals are observed for the three inequivalent PEt_3 ligands, again indicating stereochemical rigidity at iridium.

Summary

We have synthesized a new iridathiabenzene complex, **3**, using thiapentadienide as the source of ring carbon and sulfur atoms and exploiting C−H bond activation in the key ring-forming step. The X-ray crystal structure of this species and its solution-phase NMR spectra are consistent with the presence of an aromatic ring system in which the metal center participates in ring π-bonding. Two-electron donors such as PMe_3 and chloride react associatively with **3** at the iridium center, generating six-coordinate Ir(III) products with the iridathiacyclohexa-1,3-diene ring skeleton. This reactivity results primarily from the fact that the electrons in the Ir−S π bond of **3** can be localized on sulfur, rendering the iridium atom a reactive 16e$^-$ center. Iridathiabenzene **3** also engages in a [4 + 2] cycloaddition reaction with nitrosobenzene, producing an iridathiacyclohexa-1,4-diene product. Finally, **3** behaves like a conventional arene in its reactions with organometallic reagents, forming η^6 π complexes with the $Mo(CO)_3$ and $(C_5Me_5)Ru^+$ metal−ligand fragments.

Experimental Section

General Comments. All manipulations were carried out under a nitrogen atmosphere, using either glovebox or double-manifold Schlenk techniques. Solvents were stored under nitrogen after being distilled from the appropriate drying agents. Deuterated NMR solvents were obtained from Cambridge Isotope Laboratories or from Aldrich in sealed vials and used as received. The following reagents were used as obtained from the supplier indicated: *n*-butyllithium (Aldrich), silver tetrafluoroborate (Aldrich), silver trifluoromethanesulfonate (Aldrich), bis(triphenylphosphoranylidene)ammonium chloride (PPN^+Cl^-; Aldrich), trimethylphosphine (Strem), and nitrosobenzene (Aldrich).

3,4-Dimethyl-2,5-dihydrothiophene[29] was obtained by diisobutylaluminum hydride (DIBAL-H) reduction of the corresponding sulfone.[30] $(Cl)Ir(PEt_3)_3$ was produced in situ via the reaction of $[(cyclooctene)_2IrCl]_2$ [31] with 6 equiv of PEt_3. (η^6-*p*-xylene)$Mo(CO)_3$[32] and $[(\eta^5\text{-}C_5Me_5)Ru(NCMe)_3]^+O_3SCF_3^-$ [33] were synthesized by literature procedures.

NMR experiments were performed on a Varian Unity Plus-300 spectrometer (^1H, 300 MHz; ^{13}C, 75 MHz; ^{31}P, 121 MHz), a Varian Unity Plus-500 spectrometer (^1H, 500 MHz; ^{13}C, 125 MHz; ^{31}P, 202 MHz), or a Varian Unity-600 spectrometer (^1H, 600 MHz; ^{13}C, 150 MHz; ^{31}P, 242 MHz). ^1H and ^{13}C spectra were referenced to tetramethylsilane, while ^{31}P spectra were referenced to external H_3PO_4. HMQC (^1H-detected multiple quantum coherence) and HMBC (heteronuclear multiple bond correlation) experiments aided in assigning some of the ^1H and ^{13}C peaks.

The infrared spectra were recorded on a Mattson Polaris FT IR spectrometer.

Microanalyses were performed by Galbraith Laboratories, Inc., Knoxville, TN.

Synthesis of Lithium 2,3-Dimethyl-5-thiapentadienide. 3,4-Dimethyl-2,5-dihydrothiophene (1.04 g, 9.13 mmol) was dissolved in 40 mL of tetrahydrofuran (THF) and the solution cooled to −25 °C. To this solution was added 1.67 M *n*-butyllithium in hexanes (5.8 mL, 9.28 mmol) over a 15 min period. The resulting lemon yellow solution was stirred at −25 °C for 6.5 h, followed by removal of the volatiles in vacuo, leaving an orange-brown waxy solid. To this residue was added 50 mL of pentane, and the resulting slurry was filtered through a medium-porosity frit. The collected solid was rinsed with pentane (20 and 5 mL portions) and then with diethyl ether (3 × 5 mL portions), leaving a white powder of the desired product. Yield: 0.75 g (68%).

^1H NMR (tetrahydrofuran-d_8, 22 °C): δ 6.87 (s, 1, H4), 4.87 (d, J_{H-H} = 3.0 Hz, 1, H1), 4.50 (br s, 1, H1), 2.32 (s, 3, CH_3), 1.74 (s, 3, CH_3).

Synthesis of $\overline{CH{=}C(Me)C(Me){=}CHS{=}}Ir(PEt_3)_3^+BF_4^-$ (3). Compound **4**, *mer*-$\overline{CH{=}C(Me)C(Me){=}CHS}Ir(PEt_3)_3(H)$ (0.26 g, 0.39 mmol), was dissolved in 10 mL of tetrahydrofuran (THF) and the solution cooled to −70 °C. $AgBF_4$ (0.076 g, 0.39 mmol) in 3 mL of THF was added, and the resulting solution was warmed to room temperature. After filtration, the solvent was removed in vacuo, leaving a red oil. Compound **3** was extracted from this oil with toluene and crystallized as deep red needles from toluene/pentane at −30 °C. Yield: 0.13 g (44%).

^1H NMR (acetone-d_6, 22 °C): δ 10.36 (quartet, J_{H-P} = 8.4 Hz, 1, H1), 8.61 (quartet, J_{H-P} = 3.3 Hz, 1, H4), 2.51 (s, 3, ring CH_3), 2.22 (s, 3, ring CH_3), 2.22 (d of quartets, J_{H-P} =

(29) Pettett, M. G.; Holmes, A. B. *J. Chem. Soc., Perkin Trans. 1* **1985**, 1161.

(30) Butler, G. B.; Ottenbrite, R. M. *Tetrahedron Lett.* **1967**, *48*, 4873.

(31) Herde, J. L.; Lambert, J. C.; Senoff, C. V. In *Inorganic Syntheses*; Parshall, G. W., Ed.; McGraw-Hill: New York, 1974; Vol. 15, pp 18−20.

(32) (a) Fischer, E. O.; Öfele, K.; Essler, H.; Fröhlich, W.; Mortensen, J. P.; Semmlinger, W. *Chem. Ber.* **1958**, *91*, 2763. (b) Strohmeier, W. *Chem. Ber.* **1961**, *94*, 3337.

(33) Fagan, P. J.; Ward, M. D.; Calabrese, J. C. *J. Am. Chem. Soc.* **1989**, *111*, 1698.

J_{H-H} = 7.8 Hz, 18, PEt_3 CH_2's), 0.99 (d of t, J_{H-P} = 15.6 Hz, J_{H-H} = 7.8 Hz, 27, PEt_3 CH_3's). $^{13}C\{^1H\}$ NMR (acetone-d_6, 22 °C): δ 165.1 (quartet, J_{C-P} = 21.6 Hz, C1), 143.6 (s, C2), 134.9 (s, C3), 130.0 (s, C4), 27.9 (quartet, J_{C-P} = 3.0 Hz, ring CH_3), 25.8 (s, ring CH_3), 21.1 (d, J_{C-P} = 31.5 Hz, PEt_3 CH_2's), 9.3 (quartet, J_{C-P} = 4.5 Hz, PEt_3 CH_3's). $^{31}P\{^1H\}$ NMR (acetone-d_6, 22 °C): δ 1.94 (br s). $^{31}P\{^1H\}$ NMR (acetone-d_6, −90 °C): δ 11.9 (s, 2, equatorial PEt_3's), −15.4 (s, 1, axial PEt_3).

Synthesis of *mer*-CH=C(Me)C(Me)=CHSIr(PEt$_3$)$_3$(H) (4). (Cl)Ir(PEt_3)$_3$ (2.91 g, 5.00 mmol) was dissolved in 200 mL of tetrahydrofuran (THF) and the solution cooled to −25 °C. To this solution was added lithium 2,3-dimethyl-5-thiapentadienide (0.60 g, 5.00 mmol) in 25 mL of THF dropwise over a 10 min period. After the mixture was stirred for 7 h and warmed to ambient temperature, the solvent was removed in vacuo, affording a light yellow powder. Compound **4** was extracted from this powder with 40 mL of pentane and crystallized as orange prisms from acetone at −30 °C. Yield: 2.71 g (82%).

^1H NMR (acetone-d_6, 22 °C): δ 7.05 (s, 1, H1), 5.78 (s, 1, H4), 1.90 (m, 3, ring CH_3), 1.80 (s, 3, ring CH_3), 1.95−1.60 (m, 18, PEt_3 CH_2's), 1.15−0.95 (m, 27, PEt_3 CH_3's), −16.10 (d of t, J_{H-P} = 13.2 Hz, 15.9 Hz, 1, Ir−H). $^{13}C\{^1H\}$ NMR (acetone-d_6, 22 °C): δ127.3 (s, C2), 127.3 (s, C3), 120.9 (d, J_{C-P} = 6.0 Hz, C4), 118.8 (d of t, J_{C-P} = 72.0 Hz, 15.0 Hz, C1), 28.7 (d, J_{C-P} = 9.0 Hz, ring CH_3), 26.4 (s, ring CH_3), 21.1 (d, J_{C-P} = 24.0 Hz, equatorial PEt_3 CH_2's), 17.4 (virtual t, J_{C-P} = 33.0 Hz, axial PEt_3 CH_2's), 8.6 (s, PEt_3 CH_3's). $^{31}P\{^1H\}$ NMR (acetone-d_6, 22 °C): δ −18.9 (d, J_{P-P} = 16.0 Hz, 2, axial PEt_3's), −28.3 (t, J_{P-P} = 16.0 Hz, 1, equatorial PEt_3).

Synthesis of CH=C(Me)C(Me)=CHSIr(PMe$_3$)$_4^+$BF$_4^-$ (5). Compound **3**, CH=C(Me)C(Me)=CHS=Ir(PEt_3)$_3^+BF_4^-$ (0.057 g, 0.076 mmol), was dissolved in tetrahydrofuran and the solution cooled to −30 °C. Trimethylphosphine was added dropwise with swirling until the color of the solution remained yellow. (Approximately 0.05 mL, 0.48 mmol PMe_3 was added.) After the mixture was warmed to room temperature, the volatiles were removed in vacuo. The residue was rinsed with toluene and then dissolved in acetone/diethyl ether. Cooling to −30 °C caused compound **5** to crystallize as yellow prisms. Yield: 0.040 g (75%).

^1H NMR (acetone-d_6, 22 °C): δ 6.85 (d, J_{H-P} = 14.7 Hz, 1, H1), 5.54 (d, J_{H-P} = 14.1 Hz, 1, H4), 2.09 (br s, 3, ring CH_3), 1.89 (s, 3, ring CH_3), 1.88 (d, J_{H-P} = 8.7 Hz, 9, equatorial PMe_3), 1.71 (d, J_{H-P} = 8.4 Hz, 9, equatorial PMe_3), 1.60 (virtual t, J_{H-P} = 7.2 Hz, 18, axial PMe_3's). $^{13}C\{^1H\}$ NMR (acetone-d_6, 22 °C): δ 130.2 (s, C2), 129.5 (s, C3), 116.8 (d of d, J_{C-P} = 9.0 Hz, 3.0 Hz, C4), 115.8 (d of t of d, J_{C-P} = 70.5 Hz, 12.0 Hz, 6.0 Hz, C1), 27.8 (d, J_{C-P} = 10.5 Hz, ring CH_3), 25.2 (s, ring CH_3), 19.1 (d, J_{C-P} = 30.0 Hz, equatorial PMe_3), 18.8 (d, J_{C-P} = 36.0 Hz, equatorial PMe_3), 16.1 (virtual t, J_{C-P} = 40.5 Hz, axial PMe_3's). $^{31}P\{^1H\}$ NMR (acetone-d_6, 22 °C): δ −49.9 (d of d, J_{P-P} = 20.2 Hz, 15.9 Hz, 2, axial PMe_3's), −52.0 (t of d, J_{P-P} = 20.2 Hz, 15.2 Hz, 1, equatorial PMe_3), −65.4 (t of d, J_{P-P} = 15.9 Hz, 15.2 Hz, 1, equatorial PMe_3).

Synthesis of *mer*-CH=C(Me)C(Me)=CHSIr(PEt$_3$)$_3$(Cl) (6). Compound **3**, CH=C(Me)C(Me)=CHS=Ir(PEt_3)$_3^+BF_4^-$ (0.049 g, 0.066 mmol), was dissolved in 2 mL of methylene chloride and cooled to −30 °C. PPN^+Cl^- (0.070 g, 0.12 mmol) in 3 mL of methylene chloride was added, and the resulting solution was swirled as it was warmed to room temperature. After the solution sat at room temperature overnight, the solvent was removed in vacuo. Compound **6** was extracted from the residue with pentane and crystallized as orange prisms from a concentrated pentane solution at −30 °C. Yield: 0.021 g (46%).

NMR Data for Isomer 6a. ^1H NMR (acetone-d_6, 22 °C): δ 7.92 (br s, 1, H1), 5.10 (s, 1, H4), 2.02 (obscured, ring CH_3), 1.82 (s, 3, ring CH_3), 2.15−1.95 (m, 18, PEt_3 CH_2's), 1.25−1.00 (m, 27, PEt_3 CH_3's). $^{13}C\{^1H\}$ NMR (acetone-d_6, 22 °C): δ 131.2 (d of t, J_{C-P} = 84.0 Hz, 12.0 Hz, C1), 128.0 (s, C2), 125.6 (s, C3), 114.8 (d, J_{C-P} = 6.0 Hz, C4), 26.7 (s, J_{C-P} = 9.0 Hz, ring CH_3), 25.2 (s, ring CH_3), 18.2 (d, J_{C-P} = 21.0 Hz, equatorial PEt_3 CH_2's), 14.2 (virtual t, J_{C-P} = 31.5 Hz, axial PEt_3 CH_2's), 9.0 (d, J_{C-P} = 4.5 Hz, equatorial PEt_3 CH_3's), 8.7 (virtual t, J_{C-P} = 4.5 Hz, axial PEt_3 CH_3's). $^{31}P\{^1H\}$ NMR (acetone-d_6, 22 °C): δ −32.1 (d, J_{P-P} = 16.5 Hz, 2, axial PEt_3's), −41.0 (t, J_{P-P} = 16.5 Hz, 1, equatorial PEt_3).

NMR Data for Isomer 6b. ^1H NMR (acetone-d_6, −20 °C): δ 7.43 (d, J_{H-P} = 14.7 Hz, 1, H1), 5.66 (d, J_{H-P} = 13.2 Hz, 1, H4), 1.85 (obscured, ring CH_3), 1.73 (s, 3, ring CH_3), 2.25−1.85 (m, 18, PEt_3 CH_2's), 1.30−1.00 (m, 27, PEt_3 CH_3's). $^{13}C\{^1H\}$ NMR (acetone-d_6, −20 °C): δ 128.0 (s, C2), 126.8 (s, C3), 122.1 (s, C4), 106.4 (m, C1), 27.7 (s, ring CH_3), 25.6 (s, ring CH_3), 17.1 (d, J_{C-P} = 27.8 Hz, equatorial PEt_3 CH_2's), 14.6 (virtual t, J_{C-P} = 31.5 Hz, axial PEt_3 CH_2's), 9.4 (d, J_{C-P} = 5.2 Hz, equatorial PEt_3 CH_3's), 8.8 (virtual t, J_{C-P} = 4.5 Hz, axial PEt_3 CH_3's). $^{31}P\{^1H\}$ NMR (acetone-d_6, −20 °C): δ −29.9 (d, J_{P-P} = 18.6 Hz, 2, axial PEt_3's), −32.6 (t, J_{P-P} = 18.6 Hz, 1, equatorial PEt_3).

Synthesis of [(CH=C(Me)C(Me)=CHSIr(PEt$_3$)$_2$)$_2$(μ-Cl)]$^+$-O$_3$SCF$_3^-$ (7). Compound 6, CH=C(Me)C(Me)=CHSIr(PEt_3)$_3$-(Cl) (0.050 g, 0.072 mmol), was dissolved in 7 mL of acetone, and AgO_3SCF_3 (0.008 g, 0.031 mmol, 0.43 equiv) in 1 mL of acetone was added at ambient temperature with vigorous stirring. The solution became red, and a precipitate (AgCl) formed. After it was stirred for 1 h and cooled to −30 °C, the solution was filtered. The volatiles were then removed in vacuo, and the residue was washed with three 5 mL portions of pentane to remove unreacted 6. The remaining solid was dissolved in 1:6 acetone/diethyl ether and the solution cooled to −30 °C to produce light yellow prisms. Yield: 0.033 g (84%).

^1H NMR (acetone-d_6, 22 °C): δ 8.07 (d, J_{H-P} = 9.9 Hz, 2, H1's), 5.51 (d, J_{H-P} = 11.7 Hz, 2, H4's), 2.30−1.90 (m, 24, PEt_3 CH_2's), 2.12 (s, 6, ring CH_3's), 1.75 (s, 6, ring CH_3's), 1.30−1.00 (m, 36, PEt_3 CH_3's). $^{13}C\{^1H\}$ NMR (acetone-d_6, 22 °C): δ 141.7 (s, C2's), 127.7 (s, C3's), 116.5 (s, C1's), 107.1 (s, C4's), 27.3 (s, ring CH_3's), 26.7 (s, ring CH_3's), 16.9 (filled-in d, J_{C-P} = 33.7 Hz, PEt_3 CH_2's), 16.0 (filled-in d, J_{C-P} = 31.9 Hz, PEt_3 CH_2's), 8.1 (s, PEt_3 CH_3's). $^{31}P\{^1H\}$ NMR (acetone-d_6, 22 °C): δ −12.9 (A_2X_2 pattern, 2, A-type PEt_3's), −17.6 (A_2X_2 pattern, 2, X-type PEt_3's). The four coupling constants calculated from the spectra are $J_{AA'}$ = 27.5 Hz, $J_{XX'}$ = 14.3 Hz, J_{AX} = 17.9 Hz, and $J_{AX'}$ = 3.3 Hz.

Synthesis of [CH=C(Me)C(Me)CH=SIrON(Ph)](PEt$_3$)$_3^+$-BF$_4^-$ (8). Compound **3**, CH=C(Me)C(Me)=CHS=Ir(PEt_3)$_3^+BF_4^-$ (0.040 g, 0.054 mmol), and nitrosobenzene (0.007 g, 0.065 mmol) were placed in a vial, and 5 mL of tetrahydrofuran (THF) was added at room temperature. The resulting yellow solution was stirred for 10 min before removal of the solvent in vacuo. The residue was rinsed with diethyl ether and then dissolved in THF. Addition of diethyl ether and cooling to −30 °C caused compound **8** to crystallize as a light yellow waxy solid. Yield: 0.011 g (24%).

^1H NMR (acetone-d_6, 22 °C): δ 8.31 (s, 1, H4), 7.66−7.56 (m, 5, phenyl H's), 6.79 (t, J_{H-P} = 10.0 Hz, 1, H1), 2.40−2.00 (m, 18, PEt_3 CH_2's), 1.96 (d, J_{H-P} = 1.5 Hz, 3, ring CH_3), 1.59 (d, J_{H-P} = 1.0 Hz, 3, ring CH_3), 1.40−1.00 (m, 27, PEt_3 CH_3's). $^{13}C\{^1H\}$ NMR (acetone-d_6, 22 °C): δ 154.2 (s, C4), 149.6 (d, J_{C-P} = 3.8 Hz, C2), 147.5 (s, ipso phenyl C), 136.4 (d of t, J_{C-P} = 93.0 Hz, 7.5 Hz, C1), 131.1 (s, para phenyl C), 130.5, 123.2 (s's, ortho and meta phenyl C's), 50.8 (d, J_{C-P} = 11.3 Hz, C3), 28.7 (d, J_{C-P} = 4.9 Hz, ring CH_3), 21.8 (d, J_{C-P} = 8.0 Hz, ring CH_3), 21.0 (d, J_{C-P} = 38.6 Hz, PEt_3 CH_2's), 18.2 (d, J_{C-P} = 24.0 Hz, PEt_3 CH_2's), 17.1 (d, J_{C-P} = 30.5 Hz, PEt_3 CH_2's), 9.7 (d, J_{C-P} = 6.4 Hz, PEt_3 CH_3's), 9.5 (d, J_{C-P} = 6.4 Hz, PEt_3 CH_3's),

Table 1. X-ray Diffraction Structure Summary

	3	4	6a	7	9	10
formula	$C_{24}H_{53}BF_4Ir$-P_3S	$C_{24}H_{54}IrP_3S$	$C_{24}H_{53}ClIrP_3S$	$C_{37}H_{76}ClF_3$-$Ir_2O_3P_4S_3$	$C_{27}H_{53}BF_4Ir$-MoO_3P_3S	$C_{27}H_{56}BF_4Ir$-MoO_3P_4S
fw	745.6	659.8	694.3	1265.89	925.61	959.61
cryst syst	monoclinic	monoclinic	monoclinic	triclinic	orthorhombic	monoclinic
space group	$P2_1/c$	$P2_1/n$	$P2_1/n$	$P\bar{1}$	$Pca2_1$	$P2_1$
a, Å	14.483(7)	10.416(5)	11.291(3)	10.2481(7)	19.6927(2)	10.5336(4)
b, Å	10.331(5)	16.780(4)	15.222(4)	14.8876(10)	10.4724(1)	11.8771(4)
c, Å	21.842(7)	17.166(4)	17.654(4)	17.6583(14)	36.9242(2)	15.5186(6)
α, deg	90.0	90.0	90.0	104.782(7)	90.0	90.0
β, deg	93.85(3)	90.49(3)	94.32(2)	106.746(5)	90.0	99.845(3)
γ, deg	90.0	90.0	90.0	98.483(5)	90.0	90.0
V, Å^3	3261(2)	3000.0(17)	3025.6(13)	2422.4(3)	7614.87(11)	1912.92(12)
Z	4	4	4	2	8	2
cryst dimens, mm	0.40 × 0.40 × 0.50	0.26 × 0.28 × 0.31	0.40 × 0.34 × 0.32	0.22 × 0.20 × 0.02	0.36 × 0.24 × 0.06	0.33 × 0.26 × 0.04
cryst color, habit	red prism	orange prism	orange prism	orange plate	violet plate	red plate
calcd density, g/cm^3	1.519	1.461	1.524	1.736	1.615	1.666
radiation; λ, Å	Mo Kα; 0.710 73					
temp, K	298	298	298	218(2)	218(2)	218(2)
2θ range, deg	3.0−50.0	3.0−50.0	3.0−50.0	2.54−52.00	3.88−50.00	3.92−50.00
data collected						
h	0−17	0−12	0−13	−12 to +11	0−23	−12 to +12
k	0−12	0−19	0−18	−18 to +17	0−12	−14 to +14
l	−26 to +25	−20 to +20	−21 to +20	−21 to +21	−43 to +43	0−18
total decay	none obsd					
no. of data collected	5999	5611	5647	31 280	87 736	20 917
no. of unique data	5758	5303	5359	9482	13 441	6736
Mo Kα linear abs coeff, cm^{-1}	43.41	46.90	47.39	58.49	40.46	40.70
abs cor applied	semiempirical	semiempirical	semiempirical	empirical, sadabs	empirical, sadabs	empirical, sadabs
data to param ratio	13.7:1	12.6:1	10.6:1	18.5:1	18.6:1	18.1:1
final R indices (obsd data)[a]						
R1	0.0403	0.0423	0.0385	0.0695	0.0619	0.0731
wR2	0.0553	0.0547	0.0409	0.1688	0.1300	0.1741
R indices (all data)						
R1	0.0687	0.0769	0.0912	0.1039	0.1053	0.0898
wR2	0.0664	0.0706	0.0545	0.2065	0.1493	0.1810
goodness of fit	1.00	0.89	0.98	1.072	1.028	1.035

[a] For **7**, **9**, and **10**, $I > 2\sigma(I)$; for **3**, **4**, and **6a**, $I > 3\sigma(I)$.

9.3 (d, J_{C-P} = 6.5 Hz, PEt_3 CH_3's). $^{31}P\{^1H\}$ NMR (acetone-d_6, 22 °C): δ −19.5 (dd, J_{P-P} = 15.1 Hz, 15.1 Hz, 1, PEt_3), −24.2 (dd, J_{P-P} = 15.1 Hz, 7.5 Hz, 1, PEt_3), −24.4 (dd, J_{P-P} = 15.1 Hz, 7.5 Hz, 1, PEt_3).

Synthesis of [η^6-CH=C(Me)C(Me)=CHS=Ir(PEt$_3$)$_3$]-Mo(CO)$_3^+$BF$_4^-$ (9). Compound **3**, CH=C(Me)C(Me)=CHS=Ir-$(PEt_3)_3^+BF_4^-$ (0.050 g, 0.067 mmol), and (η^6-*p*-xylene)$Mo(CO)_3$ (0.018 g, 0.063 mmol) were placed in a vial, and 6 mL of tetrahydrofuran was added at room temperature. The resulting purple solution was stirred for 1 h before removal of the solvent in vacuo. The residue was dissolved in acetone/diethyl ether and cooled to −30 °C, causing deep violet plates of compound **9** to crystallize. Yield: 0.042 g (72%).

^1H NMR (acetone-d_6, 22 °C): δ 8.27 (d of d, J_{H-P} = 15.6 Hz, 2.7 Hz, 1, H1), 6.59 (d, J_{H-P} = 9.6 Hz, 1, H4), 2.54 (s, 3, ring CH_3), 2.53 (s, 3, ring CH_3), 2.52−1.82 (m, 18, PEt_3 CH_2's), 1.44−0.98 (m, 27, PEt_3 CH_3's). $^{13}C\{^1H\}$ NMR (acetone-d_6, 22 °C): δ 220.9 (s, CO's), 129.0 (d of d, J_{C-P} = 61.8 Hz, 6.9 Hz, C1), 117.6 (s, C2), 109.5 (s, C3), 89.0 (d, J_{C-P} = 9.1 Hz, C4), 28.4 (d, J_{C-P} = 4.5 Hz, ring CH_3), 24.9 (d, J_{C-P} = 34.3 Hz, PEt_3 CH_2's), 24.4 (s, ring CH_3), 20.6 (d, J_{C-P} = 32.1 Hz, PEt_3 CH_2's), 20.3 (d, J_{C-P} = 25.2 Hz, PEt_3 CH_2's), 10.4 (d, J_{C-P} = 6.7 Hz, PEt_3 CH_3's), 9.9 (d, J_{C-P} = 6.9 Hz, PEt_3 CH_3's), 9.6 (d, J_{C-P} = 6.9 Hz, PEt_3 CH_3's). $^{31}P\{^1H\}$ NMR (acetone-d_6, 22 °C): δ 32.2 (d, J_{P-P} = 12.2 Hz, 1, axial PEt_3), −14.6 (d of d, J_{P-P} = 20.1 Hz, 12.2 Hz, 1, basal PEt_3), −28.6 (d, J_{P-P} = 20.1 Hz, 1, basal PEt_3).

Synthesis of [η^4-CH=C(Me)C(Me)=CHS=Ir(PEt$_3$)$_2$(CO)]-Mo(PMe$_3$)$_2$(CO)$_2$ (10). Compound **9**, [η^6-CH=C(Me)C(Me)=CHS=Ir$(PEt_3)_3$]$Mo(CO)_3^+BF_4^-$ (0.033 g, 0.036 mmol), was dissolved in 5 mL of acetone, producing a dark purple solution. At ambient temperature, PMe_3 (0.010 g, 0.13 mmol) in 7 mL of acetone was added to this solution with stirring, causing the color to change to dark red. After the mixture was stirred for an additional 1 h, the volatiles were removed in vacuo, leaving a red oil. This residue was dissolved in acetone/diethyl ether and the solution cooled to −30 °C, causing deep red plates of **10** to crystallize. Yield: 0.017 g (50%).

^1H NMR (acetone-d_6, 22 °C): δ 7.60 (s, 1, H1), 5.92 (s, 1, H4), 2.50−2.00 (m, 12, PEt_3 CH_2's), 1.96 (s, 3, ring CH_3), 1.89 (d, J_{H-P} = 7.8 Hz, 9, PMe_3), 1.87 (s, 3, ring CH_3), 1.52 (d, J_{H-P} = 7.8 Hz, 9, PMe_3), 1.30−1.10 (m, 18, PEt_3 CH_3's). $^{13}C\{^1H\}$ NMR (acetone-d_6, 22 °C): δ 235.0 (d, J_{C-P} = 29.1 Hz, CO on Mo), 232.1 (m, CO on Mo), 176.7 (t, J_{C-P} = 7.2 Hz, CO on Ir), 148.6 (s, C2), 138.5 (d, J_{C-P} = 70.3 Hz, C1), 121.1 (s, C3), 116.0 (m, C4), 25.8 (d, J_{C-P} = 4.5 Hz, ring CH_3), 22.4 (d, J_{C-P} = 31.6 Hz, PEt_3 CH_2's), 20.9 (s, ring CH_3), 19.4 (d, J_{C-P} = 29.1 Hz, PEt_3 CH_2's), 19.0 (d, J_{C-P} = 24.3 Hz, PMe_3), 18.3 (d, J_{C-P} = 26.1 Hz, PMe_3), 8.6 (d, J_{C-P} = 4.8 Hz, PEt_3 CH_3's), 7.5 (d, J_{C-P} = 4.2 Hz, PEt_3 CH_3's). $^{31}P\{^1H\}$ NMR (acetone-d_6, 22 °C): δ 7.6 (d, J_{P-P} = 14.5 Hz, 1, axial PEt_3), −0.5 (dd, J_{P-P} = 43.2 Hz, 14.5 Hz, 1, PMe_3), −19.4 (d, J_{P-P} = 43.2 Hz, 1, PMe_3), −29.0 (s, 1, basal PEt_3).

Synthesis of [η^6-CH=C(Me)C(Me)=CHS=Ir(PEt$_3$)$_3$]-Ru(η^5-C$_5$Me$_5$)$^{2+}$BF$_4^-$O$_3$SCF$_3^-$ (11). Compound **3**, CH=C(Me)C-(Me)=CHS=Ir$(PEt_3)_3^+BF_4^-$ (0.044 g, 0.059 mmol), was dissolved in 2 mL of acetone and cooled to −30 °C. This solution was then added to a cold (−30 °C), stirred solution of (η^5-C_5-

$Me_5)Ru(NCMe)_3^+O_3SCF_3^-$ (0.028 g, 0.055 mmol) in 10 mL of acetone. The resulting solution was warmed to ambient temperature and stirred for an additional 1 h, during which time the color changed from burgundy to orange-red. Filtration, followed by removal of the volatiles in vacuo, resulted in an orange film of **11**. Yield: 0.058 g (94%).

^{1}H NMR (acetone-d_6, 22 °C): δ 8.83 (d of t, J_{H-P} = 15.6 Hz, 3.0 Hz, 1, H1), 6.63 (d, J_{H-P} = 9.0 Hz, 1, H4), 2.47 (s, 3, ring CH_3), 2.43 (s, 3, ring CH_3), 2.60−1.80 (m, 18, PEt_3 CH_2's), 1.94 (s, 15, cyclopentadienyl CH_3's), 1.46 (d of t, J_{H-P} = 14.7 Hz, J_{H-H} = 7.4 Hz, 9, PEt_3 CH_3's), 1.36 (d of t, J_{H-P} = 14.7 Hz, J_{H-H} = 7.4 Hz, 9, PEt_3 CH_3's), 0.94 (d of t, J_{H-P} = 17.7 Hz, J_{H-H} = 7.5 Hz, 9, PEt_3 CH_3's). ^{13}C{^{1}H} NMR (acetone-d_6, 22 °C): δ 116.8 (d of d, J_{C-P} = 62.7 Hz, 6.8 Hz, C1), 110.6 (s, C2), 100.5 (s, C3), 99.0 (s, cyclopentadienyl C's), 77.9 (d, J_{C-P} = 7.6 Hz, C4), 24.8 (d, J_{C-P} = 36.2 Hz, PEt_3 CH_2's), 23.9 (d, J_{C-P} = 4.5 Hz, ring CH_3), 21.9 (d, J_{C-P} = 30.2 Hz, PEt_3 CH_2's), 20.6 (d, J_{C-P} = 25.7 Hz, PEt_3 CH_2's), 20.0 (s, ring CH_3), 11.0 (d, J_{C-P} = 7.6 Hz, PEt_3 CH_3's), 10.7 (s, cyclopentadienyl CH_3's), 10.3 (d, J_{C-P} = 6.0 Hz, PEt_3 CH_3's), 9.7 (d, J_{C-P} = 6.0 Hz, PEt_3 CH_3's). ^{31}P{^{1}H} NMR (acetone-d_6, 22 °C): δ 30.1 (d, J_{P-P} = 11.4 Hz, 1, axial PEt_3), −10.3 (d of d, J_{P-P} = 18.3 Hz, 11.4 Hz, 1, basal PEt_3), −22.5 (d, J_{P-P} = 18.3 Hz, 1, basal PEt_3).

X-ray Diffraction Studies of [CH=C(Me)C(Me)=CHS=Ir(PEt$_3$)$_3$]$^+$BF$_4^-$ (3), *mer*-CH=C(Me)C(Me)=CHSIr(PEt$_3$)$_3$(H) (4), *mer*-CH=C(Me)C(Me)=CHSIr(PEt$_3$)$_3$(Cl) (6a), [(CH=C(Me)C(Me)=CHSIr(PEt$_3$)$_2$)$_2$(μ-Cl)]$^+$O$_3$SCF$_3^-$ (7), [η^6-CH=C(Me)C(Me)=CHS=Ir(PEt$_3$)$_3$]Mo(CO)$_3^+$BF$_4^-$ (9), and [η^4-CH=C(Me)C(Me)=CHS=Ir(PEt$_3$)$_2$(CO)]Mo(PMe$_3$)$_2$(CO)$_2^+$BF$_4^-$ (10). Single crystals of compounds **3**, **4**, **6a**, **7**, **9**, and **10** were either sealed in a glass capillary or mounted on a glass fiber under a nitrogen atmosphere. X-ray data for **3**, **4**, and **6a** were collected on a Siemens R3m/V diffractometer at room temperature, while data for **7**, **9**, and **10** were obtained using a Bruker SMART charge coupled device (CCD) detector system at 218 K. In each case, graphite-monochromated Mo Kα radiation was supplied by a sealed-tube X-ray source.

Structure solution and refinement were carried out using the SHELXTL-PLUS software package (PC version).[34] The iridium atom positions were determined by direct methods. The remaining non-hydrogen atoms were found by successive full-matrix least-squares refinement and difference Fourier map calculations. In general, non-hydrogen atoms were refined anisotropically, while hydrogen atoms were placed at idealized positions and assumed the riding model.

Crystal data and details of both collection and structure analysis are listed in Table 1.

Dynamic NMR Studies. Determination of $\Delta G^\ddagger$ for the Fluxional Process Exhibited by 3. ^{31}P{^{1}H} NMR spectra were recorded at 10 °C intervals over the temperature range where fluxional behavior was exhibited (+10 °C → −80 °C). Theoretical line shapes were calculated for a series of rates using the method of Johnson.[35,36] The experimental spectra were then matched against the theoretical spectra, and in this way, exchange rate constants were determined for each temperature. These exchange rate constants, k, were used to calculate the free energy of activation, $\Delta G^\ddagger$, at each temperature, T, using the Eyring equation. The reported $\Delta G^\ddagger$ is the average value over all of the temperatures in the simulation, and the uncertainty is the estimated standard deviation.

Acknowledgment. Support from the National Science Foundation and the donors of the Petroleum Research Fund, administered by the American Chemical Society, is gratefully acknowledged. We also thank Johnson Matthey Alfa/Aesar for a loan of $IrCl_3 \cdot 3H_2O$. Washington University's High Resolution NMR Service Facility was funded in part by NIH Support Instrument Grants (Nos. RR-02004, RR-05018, and RR-07155).

Supporting Information Available: Structure determination summaries and listings of final atomic coordinates, thermal parameters, bond lengths, and bond angles for compounds **3**, **4**, **6a**, **7**, **9**, and **10** and a summary of analytical data. This material is available free of charge via the Internet at http://pubs.acs.org.

OM010050S

(34) Sheldrick, G. M. Bruker Analytical X-ray Division, Madison, WI, 1997.
(35) Johnson, C. S., Jr. *Am. J. Phys.* **1967**, *35*, 929.
(36) Martin, M. L.; Martin, G. J.; Delpuech, J.-J. *Practical NMR Spectroscopy*; Heydon: London, 1980; pp 303−309.